JAERI-M
91-217

EXPERIMENTAL DATA REPORT FOR TEST TS-1

REACTIVITY INITIATED ACCIDENT TEST IN NSRR

WITH PRE-IRRADIATED BWR FUEL ROD

January 1992

Takehiko NAKAMURA, Makio YOSHINAGA, Makoto SOBAJIMA,
Toshio FUJISHIRO, Ohichiro HORIKI, Takeshi YAMAHARA,
Yoshinori ICHIHASHI and Teruo KIKUCHI

日 本 原 子 力 研 究 所
Japan Atomic Energy Research Institute

Experimental Data Report for Test TS-1

Reactivity Initiated Accident Test in NSRR

with Pre-irradiated BWR Fuel Rod

Takehiko NAKAMURA, Makio YOSHINAGA, Makoto SOBAJIMA

Toshio FUJISHIRO, Ohichiro HORIKI, Takeshi YAMAHARA[+]

Yoshinori ICHIHASHI[+] and Teruo KIKUCHI[+]

Department of Fuel Safety Research

Tokai Research Establishment

Japan Atomic Energy Research Institute

Tokai-mura, Naka-gun, Ibaraki-ken

This report presents experimental data for Test TS-1 which was the first in a series of tests, simulating Reactivity Initiated Accident (RIA) conditions using pre-irradiated BWR fuel rods, performed in the Nuclear Safety Research Reactor (NSRR) in October, 1989.

Test fuel rod used in the Test TS-1 was a short-sized BWR(7×7) type rod which was fabricated from a commercial rod provided from Tsuruga Unit 1 power reactor. The fuel had an initial enrichment of 2.79% and burnup of 21.3 GWd/t (bundle average).

Pulse irradiation was performed at a condition of stagnant water cooling, atmospheric pressure and ambient temperature using a newly developed double container-type capsule. Energy deposition of the rod in this test was evaluated to be about 61 cal/g·fuel (55 cal/g·fuel in peak fuel enthalpy) and no fuel failure was observed.

Descriptions on test conditions, test procedures, fuel burnup measurements[1], transient behavior of the test rod during pulse irradiation

---

Note: (1) Fuel burnup and energy deposition by the pulse irradiation was evaluated in co-operation with Department of Chemistry.

+ Department of Hot Laboratories

and results of post pulse irradiation examinations are contained in this
report.

実験データレポートTest TS-1

照射済ＢＷＲ燃料を用いた反応度事故実験

日本原子力研究所東海研究所燃料安全工学部

中村　武彦　・吉永真希夫　・傍島　　眞

藤城　俊夫　・堀木欧一郎　・山原　　武[+]

市橋　芳徳[+]・菊池　輝男[+]

　本報告書は，1989年10月に実施した照射済ＢＷＲ燃料を用いた最初の反応度事故模擬実験である
TS-1について，実験データをまとめたものである。

　TS-1実験に使用した試験燃料は，初期濃縮度2.79％であり，敦賀１号炉で照射されたＢＷＲ７×
７型燃料棒を短尺化したものである。短尺化に供した実用燃料のバンドル平均燃焼度は21.3GWd／t
であった。

　ＮＳＲＲにおける照射実験は，新たに開発した専用の二重カプセルを用い，大気圧・室温の静止
水冷却条件下で行い，発熱量61cal／g・fuel（ピークエンタルピ55cal／g・fuel）を与えた。その結
果，燃料破損は生じなかった。

　実験条件，実験方法，燃料燃焼度の測定結果[1]，パルス照射時の燃料の過渡挙動及び照射後検
査の結果をまとめて示した。

目　　　　次

Contents

1. Introduction

Inpile fuel behavior tests with pre-irradiated fuel rods simulating RIAs (Reactivity Initiated Accidents) have started in the NSRR (Nuclear Safety Research Reactor), at JAERI in the middle of 1989, following a decade of research on the fresh fuel performance at the accident conditions (Phase I). Test fuel rods used in the new experiments (Phase II) include,

(1) Short sized fuel rods refabricated from the long sized fuel rods provided from commercial power reactors (PWRs and BWRs), and,
(2) Short sized fuel rods pre-irradiated in the Japan Material Testing Reactor (JMTR).

The short sized fuel rods for the BWR rod tests were fabricated from a commercial fuel rod which was irradiated at Tsuruga Unit 1 power reactor from 1972 to 1978 (6 cycles). The long sized commercial rod had an bundle average burnup of 21.3 GWd/t. Each of the test rods fabricated from the long-sized rod contained 6 UO_2 pellets with dishes. The initial enrichment of the fuel was 2.79%. The test rods were taken from a part where fuel burnup was fairly flat.

In the past, tests simulating RIAs with pre-irradiated fuels were performed in the SPERT[1],[2] and PBF[3],[4] projects of the United States. In the SPERT project, 10 tests using pre-irradiated fuel rods of burnups ranging from 0.99 to 32.7 GWd/t were performed at conditions simulating BWR cold start-ups. Maximum fuel enthalpies ranged from 137 to 282 cal/g·UO_2 in the tests. Fuel failure was observed in tests in which peak fuel enthalpy reached higher than 143 cal/g·UO_2. However, in a test, No.859 of the SPERT project, the fuel rod with a burnup of 31.8 GWd/t was found to have failed at the enthalpy of 85 cal/g·UO_2 early during pulse irradiation on the way to reach the peak fuel enthalpy of 154 cal/g·UO_2. The failure energy was considerably lower than those observed in the other tests (143 cal/g·UO_2 or higher). The mechanism of the low energy failure in the test 859 has been considered to be Pellet Cladding Mechanical Interaction (PCMI).

Three other RIA tests, using a cluster of 4 fuel rods of relatively low burnups ranging from 4.43 to 5.3 GWd/t under conditions simulating BWR hot start-ups, were performed in the PBF project. Three of the four fuel rods survived in a test, named RIA 1-2, at a radial average enthalpy of 185 cal/g·UO_2, only one fuel rod failed at the same enthalpy in the test. Two other test were performed at higher energies to investigate mechanical energy generation associated with fuel failure.

MacDonald et al.[5] have reviewed the results of the two projects, and concluded that the high strain rate deformation of relatively cold irradiated cladding could result in a cladding fracture at a radial average fuel enthalpy of about 140 cal/g·UO$_2$. Another type of cladding fracture during quenching of cladding, which experienced high temperature near the melting temperature and subsequent thickening and thinning, can occur when the radial peak fuel enthalpy reached 250 cal/g·UO$_2$. However, because only limited data were available for safety evaluation, the performance of pre-irradiated fuel rods at RIA conditions including effects of burnups has not been clearly understood. The objectives of the phase II program with pre-irradiated fuels are,

(1) to determine the failure thresholds of pre-irradiated fuels with the parameters of fuel burnup, initial rod power and so on,
(2) to clarify the failure modes and failure mechanisms of pre-irradiated fuels, and,
(3) to clarify the consequences of the failure of pre-irradiated fuels.

The results obtained from phase II program will reinforce experimental data base for the safety evaluation guidelines. The first test using pre-irradiated BWR fuel, Test TS-1, was successfully performed on the 24th of October, 1989. The test fuel rod was subjected to an energy deposition of about 61 cal/g·fuel. The radially averaged peak fuel enthalpy was estimated to be 55 cal/g·fuel. This report presents test conditions, test procedures, fuel burnup measurements , transient behavior of the test rod during pulse irradiation and results of post pulse irradiation examinations of the Test TS-1.

2. NSRR Facility

The NSRR is a modified TRIGA-Annular Core Pulse Reactor (ACPR) utilizing uranium-zirconium hydride (U-ZrH) fuel-moderator elements. The reactor has a dry experimental cavity (experimental tube) of 22 cm in inner diameter penetrating the core center. Test fuel rods contained in an experimental capsule are installed in the experimental tube and exposed to a high pulsed neutron flux simulating RIA conditions. The core structure is located at the bottom of 9 m deep open pool, as is shown in Fig. 1, and is cooled by natural circulation of the pool water. The NSRR was designed exclusively to conduct power transient experiments and attained its first criticality in May, 1975. The characteristics of the reactor was reported in Ref. 6 by Saito et al.

The NSRR core configuration is illustrated in Fig. 2. The core contains 149 driver fuel-moderator elements, 6 fuel follower regulating rods and 2 fuel follower safety rods, making 157 driver fuel elements in total. In addition, three transient rods with air filled followers are used to insert reactivities for pulsing operations. The regulating rods and the safety rods are driven electrically, and the transient rods are driven pneumatically. These rods are arranged to form a hexagonal pattern surrounding the experimental tube. The active zone of the fuel-moderator element is 38.1 cm long and 3.56 cm in diameter in which ZrH moderator (88%ZrH) is homogeneously combined with enriched Uranium fuel (12%U). The Uranium is enriched to 20% in ^{235}U and the H to Zr atom ratio of the ZrH moderator is 1.6. The pulsing power escalation is controlled by spectrum hardening caused by moderator temperature increase, in addition to the Doppler effect in the NSRR. The characteristics of the NSRR is listed in Table 1.

Since a modification of the operating system in fiscal year 1988, the NSRR has been operated in four modes as is shown in Table 2. Steady state operation of a power up to 300 kW is controlled by adjusting a bank of regulating rod position. High power operations up to 10MW in Shaped Pulse and Combined Pulse modes are achieved by rather quick operations of the regulating rods (at a speed of up to 75mm/s). The reactor energy release is limited within 110MWs in the two modes. Pulsings from 0 and rated powers are realized by quick withdrawals of the three transient rods in Natural Pulse mode and Combined Pulse mode, respectively. The maximum reactivity insertion of $4.7 from zero power is allowed to produce peak reactor power of 23,000MW and reactor energy release of 130MWs for the pulsing operation.

3. Test Conditions

3.1 Test Fuel Rod

3.1.1 Design

A short sized BWR 7x7 type fuel rod which contained 6 UO_2 pellets was pulse-irradiated in the Test TS-1. Structure of the rod is illustrated in Fig. 3. The test fuel rod consisted of irradiated pellet stack of about 126mm long in the middle surrounded by the original irradiated cladding, an newly made upper structure and a bottom structure welded to the irradiated fuel rod, making 304mm long (nominal) test fuel rod.

The upper structure had a gas plenum consisted of a spring, a electromagnetic core to measure pellet stack longitudinal movement and aluminum pellets leading pellet stack movement to the core and for thermal insulation. A movement marker, to record maximum pellet stack elongation relative to cladding, was placed in an open space on the top of fuel stack next to a Hafnium (Hf) disk which was installed to avoid power peaks at the ends of the fuel stack. The lower structure consisted of a strain gauge type pressure sensor made of Zircaloy. Another Hf disk, an aluminum pellet and a spacer having a center hall to have a good gas conductance were placed between the fuel stack and the pressure sensor at the bottom of the test fuel rod.

A fuel segment about 1,000mm from top end of a long sized commercial fuel, JAB73/B6, was used for the fabrication of the short sized fuel rod for the Test TS-1. Gamma scanning profile of the long sized rod and segmented locations are shown in Fig. 4. The test rod was filled with a mixture gas of Xe, Kr and He at a fraction of 77.9, 11.3, 10.8%, respectively, which simulated End Of Life (EOL) gas content of the mother rod. Fabrication of the test rod was made at Fuel Examination Facility at JAERI Tokai. Appearance of the test fuel rod used in the Test TS-1 is shown in Photo. 1. Major characteristics of the fuel rod are listed in Table 3.

3.1.2 Irradiation in Power Reactor

The mother rod, JAB73/B6, was one of the first fuel rods fabricated with domestically made cladding tubes and used in commercial reactors. Series of comprehensive Post Irradiation Examinations (PIEs) were performed to the sister rods by Tsuchie et al.[7]-[10] The cladding tube of the rods in the

assembly JAB73 was fabricated by Sumitomo Metal Industry Co. The major characteristics of the cladding tube are listed in Table 4[7]. The rod B6 of the assembly JAB73 contained fuel pellets with dishes, 21mm in height, 12.37mm in diameter and 2.79% at ^{235}U enrichment without additives. Fuel design characteristics are listed in Table 5[7].

The assembly was loaded to Tsuruga Unit 1 power reactor and irradiated from 1972 to 1978 for 6 cycles, as is shown in Fig. 5[7]. The reactor was operated following IOMR (Interim Operating Management Recommendation) for the first cycle, and PCIOMR (Pre-Conditioning Interim Operating Management Recommendation) for the rest of the irradiation cycles. The tested fuel rod, B6, location in the bundle, JAB73, is shown in Fig. 6[7]. The bundle average burnup of the assembly JAB73 was estimated[7] as 21.3GWd/t. Average burnups of the rods consisting the assembly JAB73 varies from 16 to 26GWd/t. The burnup of the rod B6 was estimated to be 22GWd/t by fission product measurements which is described later in section 5. Major irradiation conditions of the rod B6 were estimated, as follows,

Local peak burnup   26GWd/t,
Rod average burnup   22GWd/t,
Peak linear heat generation rate   330W/cm,
Rod average heat generation rate   270W/cm, and
Fast Neutron Fluence $3\text{-}4 \times 10^{21}$n/cm^2 [7] (E>1MeV, Bundle average).

3.1.3 Post Irradiation Examinations (Before Pulse Irradiation)

Series of non-destructive tests, including visual inspections, profile measurement, X-ray radiography, γ - scanning, etc., on the commercial rod, JAB73/B6, were performed. Cutting locations were decided based on these test results. Pieces of fuel rod samples were taken for PIEs from the commercial rod as well as fuel segments for fabrication of test fuel rods. Sampling locations of the segment for test TS-1 and for PIEs are shown in Fig. 7 on a diameter profile map of the rod JAB73/B6, in addition to the Fig. 4 on the γ - scanning profile map. The γ - scanning profile shown in the Fig. 4 suggests a constant fuel burnup over the segmented section. An gas puncturing test conducted prior to the segmentation of the mother rod JAB73/B6 indicated the gap gas condition listed in Table 6. A fission product inventory calculation with ORIGIN-2 code at a burnup of 22GWd/t resulted in gas amounts of 1.30×10^{-2} and 1.18×10^{-1} mols for Kripton (Kr) and Xenon (Xe), respectively. Rod average Fractional Gas Releases (FGRs) of Kr

and Xe are then estimated to be 17.9% and 16.6%, respectively.

The test fuel rod for the Test TS-1, called B6-1 or later numbered 01NJJB01, have examined by the following non-destructive tests before the pulse irradiation.

(1) X-ray radiography,

(2) γ -scanning,

(3) Profile measurement (diameter, bowing), and

(4) Eddy current test.

Fuel and cladding samples were taken from the neighboring section of fuel rod JAB73/B6 for destructive tests, such as,

(5) Metallography,

(6) SEM/EPMA,

(7) X-ray diffraction analysis,

(8) α · β γ autoradiography,

(9) Micro γ scanning,

(10)Cladding hardness measurement, and

(11)Hydrogen measurement.

Results of these PIEs are described in the following section.

(1) X-ray radiography

Two X-ray radiographs from angle 0 and 90 degrees are shown in Photo. 2. The angle which facing to the core center during irradiation in the commercial reactor was defined as 0 degree. Location of the movement maker before the pulse irradiation is identified at the top of the fuel stack.

(2) γ - scanning

Longitudinal intensity profile of gamma peaks from Caesium (Cs)-137, Zirconium (Zr)-95, Cs 134, Europium (Eu)-154 were measured using a collimator with a 0.5mm wide window, as is shown in Fig. 8. Gamma energies of the measured peaks were 662, 724, 794, 1274 keV for Cs-137, Zr-95, Cs-134 and Eu-154, respectively. Clear peaks were seen in the Cs-137 profile at pellet-pellet interfaces. Countings were smaller and no special tendency was seen in the other profiles.

Gamma spectroscopies of the mother rod were conducted at three locations, namely at 156mm from the top (gas plenum), at 2138mm (pellet

midpoint) and at 2402mm (pellet interface where maximum of Cs-137 peak was observed). A peak from Kripton (Kr) 85 is seen in Fig. 9, in addition to peaks from Cs-137 and Co-60. No qualitative difference were observed in the γ peaks at two locations of the fuel pellet. Peaks from Cs-134, Cs-137, Eu-154, Co-60, and probable Pr-144 were found at the two locations. Peaks identified are listed below.

Nuclides	Energy(keV)	Nuclides	Energy(keV)
Cs-134	563.3	Eu-154	723.8
	604.5		756.6
	801.9		873.1
	795.5		996.6
	1038.4		1004.9
	1167.9		1275.0
			1597.3
Cs-137	661.7		
		Co-60	1173.2
Pr-144	692.7		1332.5
	1493.9		

Gamma peaks at 568.9 and 904.0 keV remained unknown.

(3) Profile measurement (diameter, bowing)

Overall length, excluding the top end projection of the test fuel rod for the Test TS-1, was measured as 306.61 mm. Diametral profile at two angles and bowing to the angle which showed maximum bending were also measured, as is shown in Fig. 10. The maximum and minimum diameter of the original irradiated cladding were 14.39 and 14.19 mm, respectively, while the original diameter was 14.3 mm nominal. The maximum bowing was 0.12mm to angle 30 degrees.

(4) Eddy current test

The TS-1 test rod was examined by eddy current test at two frequencies of 64 and 512 kHz for X_1-Y_1 and X_2-Y_2 measurements. Phase angles for the two measurements were 155 and 340 degrees, respectively. Components shown as X_3 and Y_3 in Fig. 11 were obtained as sums of those of suffixes 1 and 2, $X_3 = X_1 + X_2$ for example. No major defects were identified by this eddy current test.

(5) Metallography

Two metallography samples, MCl(radial cross section) and ML (axial cross section), were taken from the mother rod about 2,200 mm from the top, as is

shown in Figs. 4 and 7. Photographs 3 and 4 shows macroscopic views of the two samples as polished. A faint ring inside the darker outer half, called porous annulus, is seen at intermediate zone of the radial cross section sample. The ring was also observed in sister rods[1] irradiated at higher heat rate and obtained fuel burnups of about 20 GWd/t or higher.

Enlarged views of the radial cross section sample as polished and as etched are shown in Photo. 5. Pellet structure and grain growth of the MC1 sample as etched are shown in micrographs of three typical areas, central zone, intermediate zone and periphery, in Photo. 6. Average grain diameters of the three zones were evaluated to be 11.5, 5.2 and 5.1 μ m for central, intermediate and peripheral zones, respectively. The diameters were averages of equivalent grain diameters in zones of 150 X 150 μ m^2. The equivalent diameters were obtained as diameters of the circles of equal areas to the grains. Average grain diameters of the axial cross section sample (ML) at four zones, central, intermediate 1, intermediate 2 and peripheral, were evaluated to be 10.1, 8.9, 6.5 and 6.4 μ m.

Nodular corrosions were found on the outer surfaces of the cladding of the two cross sectional samples. An example on the radial cross section sample (MC1) is shown in Photo. 7. The thickness of the corrosions varied from 35.3 to 63.3 μ m. Thin oxide layers of 4.4 to 5.4 μ m thick were also found on the inner surface at a few locations, as is shown in Photo. 8. A nodular corrosion found on the ML sample was 62.1 μ m thick. Thin layers of oxides of 3.6 to 6.1 μ m thick were also found on the both surfaces at some locations. Distributions of hydrides in the cladding were examined with the two samples as were etched. Photograph 9 shows the hydride distributions accompanied by micrographs of cladding grain observation .

(6) SEM/EPMA

Elemental analyses by Electron Probe Micro Analyser (EPMA) at four locations of radial cross section sample MC2, which was taken from a fuel adjacent to MC1 and coated with carbon, were performed. No other element than Uranium (U), Oxygen (O), Carbon (C) and Sulfur (S) was found at center and periphery of the fuel pellet, where S was judged to be oil of a diffusion vacuum pump of the analyser. Zirconium (Zr) and Tin (Sn) were also found, in addition to O, S and C, at an oxide layer on the inner surface where a bonding of the pellet and cladding was occurred. Fission product Caesium (Cs) and Rubidium (Rb) were found on the fuel rich side of the bonding. Line analysis results of U, O, Zr, Cs and Rb were shown in Photo. 10 on the Secondary Electron Microscopy (SEM) images of the bonding. Areal distributions of the elements are shown in Photo. 11. A sharp peak is seen

at the bonding in Cs concentration distributions, while the peak for Rb concentration spreads wider inside the fuel.

(7) X-ray diffraction analysis

X-ray diffraction analysis were conducted on the sample MC2. No other peaks than from pure UO_2 were observed .

(8) α · β γ auto-radiography

Profiles of α - ray emitting nuclide distribution and β γ - ray emitting nuclide distribution were obtained by auto-radiographs of the cross section sample MC2, as are shown in Photo. 12. A thin layer of larger concentration of α emitters is seen on the outer rim of the fuel pellet. The β γ profile also shows a locally concentrated distribution. The concentration is much greater in the porous zone at outer half of the fuel cross section which looks darker in the optical micrograph in the Photo. 12.

(9) Micro γ scanning

Radial γ intensity profile at two directions of angle 0-180 degrees and 90-270 degrees were obtained for gross and Cs-137 peak. The profiles, shown in Fig. 12, indicate great depletions at the fuel center, suggesting considerable migration of Cs from the central zone to periphery. Similar tendency was observed in Cs-137 profiles of the sister rods[7] at higher burnup of 24-26 GWd/t. The depletion was not found in non-volatile Ru-106 profiles in Ref. 7.

(10) Cladding hardness measurement

Micro Vickers hardness was measured with a cladding sample from the mother rod. The Vickers hardness of the cladding ranged from 260 to 269, and the average was 264.

(11) Hydrogen measurement

Hydrogen contents in three cladding samples of the mother rod were evaluated to be from 36.8 to 37.8 ppm, averaging 37.3 ppm.

3.2 Test Capsule

A doublely sealed water capsule (type X-II) was used for the Test TS-1, which was designed exclusively for pre-irradiated BWR and PWR fuel rod tests. Configuration of the capsule is illustrated in Fig. 13. An outer capsule, 20cm in maximum diameter and 125cm in height, contains an inner capsule which serves as a pressure vessel to stand with mechanical forces which might be generated at fuel failure. Special design was made for both capsules made of stainless steel to perform the assembling and disassembling works in hot cells by remote handling. The licenced maximum fuel energy deposition in the type X-II capsule was 200 cal/g · UO_2. The test capsule, containing a test fuel rod and filled with water at ambient temperature and at atmospheric pressure was pulse irradiated in the experimental capsule of the NSRR.

3.3 Instrumentation

Major instruments to trace fuel performance during the Test TS-1 were thermocouples and a pressure sensor to measure transient fuel rod internal pressure. Six thermocouples (Pt/Pt-13%Rh, 0.2mm in diameter) were attached to the cladding surface and two other thermocouple were placed in the capsule water near the fuel surface at two locations, namely top and middle of fuel stack. The pressure sensor attached in the bottom end structure of the test fuel rod became dead during the the pulse irradiation.

A list of instrumentation applied to the test fuel rod and to the capsule is shown in Table 7. The measuring locations are illustrated in Fig. 14. A pressure sensor for capsule pressure measurement was attached to the bottom end of fuel supporting rods. A gauge for capsule strain measurement was attached on the inner capsule flange.

3.4 Test Procedure

A rough flow of the experimental procedure is illustrated in Fig. 15. The test fuel rod was fabricated from the mother rod, JAB73/B6, at Large Hot Laboratory at JAERI Tokai. The fabrication procedure of PWR type short sized rods was reported in Ref. 11. The procedure for the BWR type rods was quite similar.

The fuel rod transferred to the NSRR was instrumented in an iron cell with special instrumentation devices. The instrumented test fuel rod,

attached to a fuel supporting rod connecting to a capsule flange shown in Photo. 13, was assembled into the test capsules in a hot cave. The inner capsule contained the test fuel rod was filled with water at ambient temperature and closed leak tight with cover gas of helium at atmospheric pressure. Tightness for fission product leakage was examined by helium leak tests of inner and outer teat capsule. The assembling of the test capsule needed roughly a month.

The capsule was then transferred in the experimental tube with a loading device equiped with radiation shields and instrumentation cable connections. The test fuel rod contained in the capsule was pulse irradiated by a natural pulse operation at a reactivity insertion of $ 3.68 nominal. The pulse irradiation was performed at acondition of stagnant water cooling, atmospheric pressure and ambient temperature. The pulse irradiation was performed at 14:25 of October 24, 1989. Irradiation conditions are summarized in Table 8.

The inner capsule was transferred to another hot laboratory, Research Hot Laboratory in JAERI Tokai, after the outer capsule was disassembled in the NSRR. Most of the post pulse-irradiation examinations were performed there. A fuel solution sample was transferred to Department of Chemistry for burnup measurements about 43 days after the pulse irradiation.

4. Transient Behavior during Pulse Irradiation

Transient responses of the thermocouples on the cladding surface were shown in Fig. 16. Thermocouple #1 became dead at the time of pulse irradiation. The maximum temperature recorded was about 100 ℃, except for the thermocouple #5 which recorded a maximum of 65 ℃. No Departure from Nucleate Boiling (DNB) was observed in the test. A thermocouple, located near fuel stack center in the water at a distance of 10 mm from cladding surface, indicated maximum temperature of about 40 ℃ and showed periodical temperature rise to 40 - 30 ℃, as is shown in Fig. 17. Another thermocouple located at the top of fuel rod showed a delayed temperature increase, suggesting warm water column movement by natural convection at a velocity of about 230 mm/s.

Another set of transient temperature responses of cladding surface and water in a time scale of 0 to 1 s are shown in Figs. 18 and 19, respectively. The pulsing power trace is also shown in the figures. The maximum reactor power reached approximately 9,600 MW . The pulse width at the half maximum power was about 6.7 ms. The reactor energy release, in 1 s after the pulse power was triggered, was measured as 73.5 and 74.5 MWs by micro fission chambers 1 and 2, respectively.

Transient response of the rod internal pressure sensor is shown in Fig. 20. The sensor indicated a sharp drop of the pressure by about 1.2 MPa which was slightly larger than the initial pressure difference of 1.1 MPa. The pressure trace indicated no increase by the pulse heating before it went down, and it also showed a large negative spike and stayed at a constant value after the spike. These pressure sensor response was not typical of the pre-pressurized fresh fuel at similar power transient conditions. No major defect which could cause such a quick pressure drop was found in the following post pulse irradiation examinations, including visual inspection, eddy current test and leak test which would be discussed later in section 6. Thus, the rod internal pressure sensor response was judged to be ill. Major transient records during the pulse irradiation are listed in Table 9.

5. Fuel Burnup Measurement

Amounts of fission product Barium (Ba), Neodymium (Nd), Uranium (U) and Plutonium (Pu) in samples of fuel solution were analysed to quantify the burnup of the fuel and number of additional fissions by the pulse irradiation. A fuel sample of about 2 mm thick was dissolved in Nitric Acid and transferred to Department of Chemistry for a chemical separation and analyses. Preparation procedure of the fuel solution sample is described in the section 6.

4. Transient Behavior during Pulse Irradiation

Transient responses of the thermocouples on the cladding surface were shown in Fig. 16. Thermocouple #1 became dead at the time of pulse irradiation. The maximum temperature recorded was about 100 ℃, except for the thermocouple #5 which recorded a maximum of 65 ℃. No Departure from Nucleate Boiling (DNB) was observed in the test. A thermocouple, located near fuel stack center in the water at a distance of 10 mm from cladding surface, indicated maximum temperature of about 40 ℃ and showed periodical temperature rise to 40 - 30 ℃, as is shown in Fig. 17. Another thermocouple located at the top of fuel rod showed a delayed temperature increase, suggesting warm water column movement by natural convection at a velocity of about 230 mm/s.

Another set of transient temperature responses of cladding surface and water in a time scale of 0 to 1 s are shown in Figs. 18 and 19, respectively. The pulsing power trace is also shown in the figures. The maximum reactor power reached approximately 9,600 MW . The pulse width at the half maximum power was about 6.7 ms. The reactor energy release, in 1 s after the pulse power was triggered, was measured as 73.5 and 74.5 MWs by micro fission chambers 1 and 2, respectively.

Transient response of the rod internal pressure sensor is shown in Fig. 20. The sensor indicated a sharp drop of the pressure by about 1.2 MPa which was slightly larger than the initial pressure difference of 1.1 MPa. The pressure trace indicated no increase by the pulse heating before it went down, and it also showed a large negative spike and stayed at a constant value after the spike. These pressure sensor response was not typical of the pre-pressurized fresh fuel at similar power transient conditions. No major defect which could cause such a quick pressure drop was found in the following post pulse irradiation examinations, including visual inspection, eddy current test and leak test which would be discussed later in section 6. Thus, the rod internal pressure sensor response was judged to be ill. Major transient records during the pulse irradiation are listed in Table 9.

5. Fuel Burnup Measurement

Amounts of fission product Barium (Ba), Neodymium (Nd), Uranium (U) and Plutonium (Pu) in samples of fuel solution were analysed to quantify the burnup of the fuel and number of additional fissions by the pulse irradiation. A fuel sample of about 2 mm thick was dissolved in Nitric Acid and transferred to Department of Chemistry for a chemical separation and analyses. Preparation procedure of the fuel solution sample is described in the section 6.

5.1 Fuel Burnup

Burnup of the pre-irradiated BWR fuel was evaluated from concentrations of Nd and Pu/U obtained by Mass Spectroscopy of the fuel solution. A flow of sample solution preparation is illustrated in Fig. 21. Isotopic composition of Nd, U and Pu were obtained using sample A. Concentrations of these elements were obtained using sample B with Isotope Dilution Method (IDM). Chemical separation using anion exchange technique was applied for the samples prior to the mass spectroscopy, as is shown in Fig. 22.

Isotope compositions of U, Pu and Nd are listed in Table 10. Calculated fuel burnup using Nd-148/U was 2.709 FIMA% or 26 GWd/t. FIMA is an abbreviation of Fissions Per Initial Metal Atom. The yield of Nd-148, at a fission of U-235 with a thermal neutron, is 1.671 % (when total of yields is 200%). Here, burnup was calculated with following equations,

Burnup(FIMA%) = 100 X Fission / U(Ini) ,
Fission   = Nd-148 / Y(Nd-148),
U(Ini)   = U + Pu + Fission,

where, Fission : Fission concentration (fissions/g·solution),
        Nd-148   : Nd-148 atoms concentration (atoms/g·solution),
        Y   : Fission yield (atoms/fission),
        U   : U atom concentration (atoms/g·solution),
        Pu   : Pu atom concentration (atoms/g·solution), and
        U(Ini)   : Initial U atom concentration (atoms/g·solution).

5.2 Energy Deposition by the Pulse Irradiation

Because the additional burnup by the pulse irradiation was much smaller than the burnup obtained in the commercial reactor, only a short life fission product were able to be used for evaluating number of fissions by the pulse irradiation. Fission product Barium (Ba) - 140, of a half life of 12.75 d, was chosen for the evaluation. In order to reduce high γ ray background from Cs-137 and other major fission products, chemical separation was applied to the sample solution. The separation factor was obtained by adding a known amount of Ba-133 to the solution. Amount of Ba-140 and Ba-133 were evaluated by γ spectroscopy of the sample solution from which fission products like Cs, Sr, Y, Eu, etc. were excluded by anion and cation exchange methods, as was shown in Fig. 22.

Yields producing Ba-140 by fissions of U-235, Pu-239 and Pu-241 with

thermal neutrons are 6.2, 5.4 and 5.7 %, respectively. For evaluation of the fissions in the samples, contributions of these fissile nuclides were taken account of. Atom fractions of the three fissile nuclides to the total metal atom in the solution were 0.936, 0.528 and 0.056 for U-235, Pu-239 and Pu-241, respectively. Number of fissions during the pulse irradiation was obtained with following equations,

Fission(Pls) = Ba-140 / Y(Ba-140),

$$Y(Ba\text{-}140) = \frac{U\text{-}235 \times Y(U\text{-}235) + Pu\text{-}239 \times Y(Pu\text{-}239) + Pu\text{-}241 \times Y(Pu\text{-}241)}{(U\text{-}235 + Pu\text{-}239 + Pu\text{-}241)} ,$$

where, Fission(Pls) : Fission concentration by pulse irradiation (fissions/g·solution),

Ba-140   : Ba-140 concentration at the time of pulse irradiation (atoms/g·solution),

Y(Ba-140)   : Apparent fission yield producing Ba-140 (atoms/fission),

U-235   : Atomic fraction of U-235 to total metal atoms,

Pu-239   : Atomic fraction of Pu-239 to total metal atoms,

Pu-241   : Atomic fraction of Pu-241 to total metal atoms,

Y(U-235)   : Yield of Ba-140 by a fission of U-235 (atoms/fission),

Y(Pu-239)   : Yield of Ba-140 by a fission of Pu-239 (atoms/fission),

and

Y(Pu-241)   : Yield of Ba-140 by a fission of Pu-241. (atoms/fission)

Fission density in a unit amount of initial fuel metal is then, obtained dividing Fission(Pls) by U(Ini). Numbers of fissions during the pulse irradiation was evaluated as 1.04×10^{13} fissions/g·fuel. Assuming that 176.4 MeV out of released energy of 204 MeV was transferred into thermal energy in the test fuel by a fission in a second, energy deposition of 61 cal/g·fuel was obtained. In the NSRR project, this energy release within 1 s after the pulse was triggered has been defined as a nominal energy deposition. The total energy deposition integrated until all the fission power has been deposited, and energy deposition promptly inserted into the fuel are listed in Table 11, as well as the nominal energy deposition. The total and prompt energy depositions were evaluated as 74.1 and 55.4 cal/g·fuel, respectively. The prompt energy deposition is considered to be practically equal to the maximum fuel enthalpy taking room temperature as 0. Initial amount of UO_2 which was estimated as a sum of depleted U, produced Pu, number of fissions and Oxygen was used as the amount of fuel in the evaluations.

6. Post-Pulse Irradiation Examination

thermal neutrons are 6.2, 5.4 and 5.7 %, respectively. For evaluation of the fissions in the samples, contributions of these fissile nuclides were taken account of. Atom fractions of the three fissile nuclides to the total metal atom in the solution were 0.936, 0.528 and 0.056 for U-235, Pu-239 and Pu-241, respectively. Number of fissions during the pulse irradiation was obtained with following equations,

$$\text{Fission(Pls)} = \text{Ba-140} / \text{Y(Ba-140)},$$

$$\text{Y(Ba-140)} = \frac{\text{U-235 X Y(U-235)} + \text{Pu-239 X Y(Pu-239)} + \text{Pu-241 X Y(Pu-241)}}{(\text{U-235} + \text{Pu-239} + \text{Pu-241})} ,$$

where, Fission(Pls) : Fission concentration by pulse irradiation (fissions/g·solution),

Ba-140 : Ba-140 concentration at the time of pulse irradiation (atoms/g·solution),

Y(Ba-140) : Apparent fission yield producing Ba-140 (atoms/fission),

U-235 : Atomic fraction of U-235 to total metal atoms,

Pu-239 : Atomic fraction of Pu-239 to total metal atoms,

Pu-241 : Atomic fraction of Pu-241 to total metal atoms,

Y(U-235) : Yield of Ba-140 by a fission of U-235 (atoms/fission),

Y(Pu-239) : Yield of Ba-140 by a fission of Pu-239 (atoms/fission),

and

Y(Pu-241) : Yield of Ba-140 by a fission of Pu-241. (atoms/fission)

Fission density in a unit amount of initial fuel metal is then, obtained dividing Fission(Pls) by U(Ini). Numbers of fissions during the pulse irradiation was evaluated as 1.04×10^{13} fissions/g·fuel. Assuming that 176.4 MeV out of released energy of 204 MeV was transferred into thermal energy in the test fuel by a fission in a second, energy deposition of 61 cal/g·fuel was obtained. In the NSRR project, this energy release within 1 s after the pulse was triggered has been defined as a nominal energy deposition. The total energy deposition integrated until all the fission power has been deposited, and energy deposition promptly inserted into the fuel are listed in Table 11, as well as the nominal energy deposition. The total and prompt energy depositions were evaluated as 74.1 and 55.4 cal/g·fuel, respectively. The prompt energy deposition is considered to be practically equal to the maximum fuel enthalpy taking room temperature as 0. Initial amount of UO_2 which was estimated as a sum of depleted U, produced Pu, number of fissions and Oxygen was used as the amount of fuel in the evaluations.

6. Post-Pulse Irradiation Examination

After the pulse irradiation, the outer capsule was taken off in a hot cave in the NSRR, as was shown in Fig. 15. Then, the test fuel contained in the inner capsule was transferred to Research Hot Laboratory, JAERI Tokai. Following post-pulse examinations were performed.

Non-destructive tests
(1) Visual inspection
(2) X-ray radiography
(3) Dimensional measurement
(4) Eddy current test
(5) γ -ray measurement

Destructive tests
(1) Leak test
(2) Fuel solution preparation
(3) Metallography
(4) SEM/EPMA

6.1 Non-destructive tests

(1) Visual inspection
Visual inspections on the test capsule (inner) and the test fuel rod was performed. No apparent change was seen in the test capsule. The appearance of the test capsule irradiated in test TS-1 is shown in Photo. 13. The test fuel rod, pulse irradiated in Test TS-1, showed no obvious change in appearance. The test fuel rod appearance after the pulse irradiation is shown in Photo. 14.

(2) X-ray radiography
X-ray radiograph of the test fuel rod after the pulse irradiation was shown in Photo. 15. There was no obvious geometrical change or damage identified with the radiographs taken from two angles of 0 and 90 degrees. The gap between movement marker and the Hf disk on the top of fuel stack became wider after the transient test by about 0.3 mm to be 0.8 mm. This could mean that there was a maximum fuel stack elongation of 0.8 mm relative to the cladding during the transient irradiation. However, dimensions are not accurate in the radiographs, because the radiographs were taken using a type of point X-ray source.

(3) Dimensional measurement
Length, diameter profile and bowing of the test fuel rod was measured by a laser scanning micrometer. Total length of the rod was measured to be 306.69 mm (306.70 mm and 306.67 mm at angle 0 and 90 degrees), while the

length before the pulse irradiation was 306.61 mm. The difference of +0.08 was slightly larger than the measuring accuracy of 0.05 mm. However, taking account of the accuracy of 0.1 mm at the measurement of the initial length, this small deviation can not be concluded as a real remaining elongation.

Diameter profiles of the test fuel rod were measured at 2 directions, namely angle 0-180 and 90-270 degrees. These profiles are shown in Figs. 23 and 24, compared with those before the pulse irradiation. The profiles after the pulse irradiation were generally smaller than those before pulse irradiation. The deviations were generally smaller than 0.05 mm, but larger than the measuring accuracy of 0.005 mm. However, because the angle 0 was identified by a dimple located near a connection of the pressure sensor in the bottom end fitting, and setting of the test fuel rod was done adjusting the dimple direction visually, the angle settings before and after the pulse irradiation were not accurately the same. This could cause a slight difference in diameter profiles on the test fuel which had a slight ovality, as is shown in Fig. 7. Thus it was concluded that there was no considerable radial strain remained in the test rod in Test TS-1.

Bowing of the test fuel rod after the transient irradiation was measured at the two directions of angle 0-180 and 90-270 degrees. The maximum bowing was measured to be 0.34 mm at the angle 180 degrees. The maximum bowing was slightly larger than the one before pulse irradiation (0.12 mm at angle 30 degrees). However, because the errors caused by setting is considerably large in this bowing measurement, it was judged that no considerable additional bowing was caused by the pulse irradiation.

(4) Eddy current test

A post-pulse irradiation eddy current test was performed at a frequency of 200 kHz. Phase angle for the measurement was 67 degrees. The test result is illustrated in Fig. 25. Five minor ridge type defects were identified, but no major defect threatening integrity of the rod was found.

(5) γ -ray measurement

Longitudinal γ intensity profiles of Cs-137 peak and gross γ were measured as were shown in Figs. 26 and 27. The Cs-137 profile shows no major difference with the one before pulse irradiation shown in Fig. 8. The profile after the pulse irradiation was measured using a collimator with a 0.3 mm wide window. Gamma spectroscopies at two locations were conducted, one at a pellet-pellet interface, the other at pellet midplane.

Peaks from Ag-110m and Sb-125, in addition to those found in the spectra before pulse irradiation, were identified in the two spectra shown in Fig. 28. However, there basically is no meaningful difference in the spectra before and after the pulse irradiation.

6.2 Destructive tests

(1) Leak test

Non-destructive test results indicated no fuel failure was occurred in the Test TS-1. However, because the transient fuel rod internal pressure record showed a quick drop, the integrity of the test fuel rod was investigated further by a set of leak tests, a capsule gas sampling test and visual inspection of the pressure sensor.

A bottle of cover gas in the test capsule was sampled before the capsule was disassembled. The sampled gas, in a 300 cc stainless steel bottle of a diameter of about 50 mm and of 200 mm long, was analyzed by γ spectroscopy and mass spectroscopy. The peak of Kr-85 at 514 keV was not identified by the γ spectroscopy. Isotopes of Kr and Xe in the sampled gas were below detection limits of the mass spectrometer.

The test fuel rod was cut into two pieces at the gas plenum zone near the top end of the rod. Defect of the two fuel pieces were examined by a soap bubble test and a pressurization test in water. Photograph 13 shows test procedure for the larger bottom piece. No leakage was found in the two fuel pieces. Further more, a radiation monitor detected a considerable amount of Kr-85, when the test fuel rod had a first cut.

These test results clearly shows that no defects of the cladding, at least large defects which could cause the quick pressure drop recorded during the pulse irradiation, can't have been generated in the Test TS-1. Thus the response of the fuel internal pressure sensor was judged to be ill. In order to find the problem generated in the pressure sensor, the sensor was cut into pieces and visually inspected. No peeling off of the strain gauge in the sensor, which could cause the ill response, was recognized by the inspection. The post pulse irradiation appearance of strain gauges used for the pressure sensor is shown in Photo. 13. A clear cause for the mull-function of the pressure sensor was not found.

(2) Fuel solution preparation

A thin fuel slice of 2 mm thick was taken out of the middle part of the test fuel rod, as is shown in Fig. 29. The fuel section was filled with epoxy resin prior to the sampling to avoid any missing fuel pieces. The fuel sample was dissolved in Nitric acid being kept at a temperature of 110 ℃ for 6 h. The sampled fuel mass was estimated as 2.987 g by extracting mass of residual cladding and resin from original sample mass. A solution of 5 cc, which was 1/200 of the total solution, was transferred to the Department of Chemistry for further treatment to evaluate the fuel burnups described in section 5. The evaluated Uranium mass by the mass spectroscopy at the Department of Chemistry of 14.68 mg was slightly smaller (1.7%) than the directly estimated

mass of 14.94 mg. The dose rate of the sample at the surface of the container was 1200 μ Sv/h.

(3) Metallography

Two metallography samples, radial cross section and axial cross section, were taken from the middle part of the test rod, as is shown in Fig. 29. Photographs 14 and 15 shows macroscopic views of the two samples as polished. The macroscopic photographs shows numbers of additional cracks which mainly runs radially in the outer half of the fuel pellets.

Enlarged views of the radial cross section sample as polished and as etched at three typical areas, central zone, intermediate zone and periphery, are shown in Photo. 16. No obvious grain growth are seen in micrographs, when they are compared to those before pulse irradiation shown in Photo. 6. It is not clear from the micrographs of the polished samples shown in Photos. 6 and 16, if the microscopic cracking was occurred by the pulse irradiation or not. The photographs of etched samples cannot be used for the purpose, because apparent grain interface can be wider or narrower depending on etching conditions.

Nodular corrosions were found on the outer surfaces of the cladding of the two cross sectional samples. An example on the radial cross section sample (MC1) is shown in Photo. 17. The thickness of the corrosions ranged from 10 to 60 μ m. No significant change by the pulse irradiation in the oxide condition was recognized.

(4) SEM

Secondary Electron Microscopy (SEM) images of the fuel pellet experienced the pulse irradiation in Test TS-1 is shown in Photo. 18. Enlarged views of the grain at three typical locations as etched are also shown in the photograph.

7. Summary and Discussions

The first RIA test with pre-irradiated BWR fuel rod at the NSRR, Test TS-1, was successfully conducted. The test fuel was subjected to an energy deposition of 61 cal/g·fuel. Estimated radial average maximum fuel enthalpy was 55 cal/g·fuel. Cladding surface reached the maximum temperature of 110 °C, but no DNB (Departure from Nucleate Boiling) was observed. The test rod showed no obvious deformation nor color change by the transient. Major results from Test TS-1 are listed in Table 12.

From the metallographic examination of the pulse irradiated test fuel, numbers of macroscopic cracks were found to be generated during the pulse irradiation. The cracks run radially and located mostly in the fuel

mass of 14.94 mg. The dose rate of the sample at the surface of the container was 1200 μ Sv/h.

(3) Metallography

Two metallography samples, radial cross section and axial cross section, were taken from the middle part of the test rod, as is shown in Fig. 29. Photographs 14 and 15 shows macroscopic views of the two samples as polished. The macroscopic photographs shows numbers of additional cracks which mainly runs radially in the outer half of the fuel pellets.

Enlarged views of the radial cross section sample as polished and as etched at three typical areas, central zone, intermediate zone and periphery, are shown in Photo. 16. No obvious grain growth are seen in micrographs, when they are compared to those before pulse irradiation shown in Photo. 6. It is not clear from the micrographs of the polished samples shown in Photos. 6 and 16, if the microscopic cracking was occurred by the pulse irradiation or not. The photographs of etched samples cannot be used for the purpose, because apparent grain interface can be wider or narrower depending on etching conditions.

Nodular corrosions were found on the outer surfaces of the cladding of the two cross sectional samples. An example on the radial cross section sample (MC1) is shown in Photo. 17. The thickness of the corrosions ranged from 10 to 60 μ m. No significant change by the pulse irradiation in the oxide condition was recognized.

(4) SEM

Secondary Electron Microscopy (SEM) images of the fuel pellet experienced the pulse irradiation in Test TS-1 is shown in Photo. 18. Enlarged views of the grain at three typical locations as etched are also shown in the photograph.

7. Summary and Discussions

The first RIA test with pre-irradiated BWR fuel rod at the NSRR, Test TS-1, was successfully conducted. The test fuel was subjected to an energy deposition of 61 cal/g·fuel. Estimated radial average maximum fuel enthalpy was 55 cal/g·fuel. Cladding surface reached the maximum temperature of 110 ℃, but no DNB (Departure from Nucleate Boiling) was observed. The test rod showed no obvious deformation nor color change by the transient. Major results from Test TS-1 are listed in Table 12.

From the metallographic examination of the pulse irradiated test fuel, numbers of macroscopic cracks were found to be generated during the pulse irradiation. The cracks run radially and located mostly in the fuel

periphery. An interesting point to look at is that if the microscopic cracking was occurred by the pulse irradiation, which could lead an additional fission product gas release in the test. Micrographs taken on the polished samples which experienced the pulse irradiation did not show a clear sign of micro cracking nor grain separation, compared with the micrographs taken on the reference sample which did not experienced a pulse irradiation. The local variation was significantly large and microscopic changes caused by the pulse irradiation was hard to be identified. A quantitative study by porosity measurement etc. is probably needed for further discussion.

8. Conclusions

The following conclusions were obtained through the Test TS-1.

(1) Fabrication of the short test fuel rod from the long commercial rod was successfully performed. The whole test, including assembling, disassembling of the test capsule and PIEs, was conducted without any major troubles. The first test using the refabricated irradiated commercial BWR rod, Test TS-1, provided useful information on fuel performance at a cold start up RIA condition.

(2) The test fuel rod experienced the quick power burst of a maximum enthalpy of 55 cal/g·fuel was still intact, showing no residual axial and radial strains. Departure from nucleate boiling did not happened, keeping the cladding surface temperature below 110 ℃. No obvious change on the cladding oxidation condition was identified.

(3) Macroscopic radial cracks at the periphery of the test fuel pellet were generated by the pulse irradiation. Grain growth and micro crackings by the pulse irradiation were not obvious.

Acknowledgement

periphery. An interesting point to look at is that if the microscopic cracking was occurred by the pulse irradiation, which could lead an additional fission product gas release in the test. Micrographs taken on the polished samples which experienced the pulse irradiation did not show a clear sign of micro cracking nor grain separation, compared with the micrographs taken on the reference sample which did not experienced a pulse irradiation. The local variation was significantly large and microscopic changes caused by the pulse irradiation was hard to be identified. A quantitative study by porosity measurement etc. is probably needed for further discussion.

8. Conclusions

The following conclusions were obtained through the Test TS-1.

(1) Fabrication of the short test fuel rod from the long commercial rod was successfully performed. The whole test, including assembling, disassembling of the test capsule and PIEs, was conducted without any major troubles. The first test using the refabricated irradiated commercial BWR rod, Test TS-1, provided useful information on fuel performance at a cold start up RIA condition.

(2) The test fuel rod experienced the quick power burst of a maximum enthalpy of 55 cal/g·fuel was still intact, showing no residual axial and radial strains. Departure from nucleate boiling did not happened, keeping the cladding surface temperature below 110 ℃. No obvious change on the cladding oxidation condition was identified.

(3) Macroscopic radial cracks at the periphery of the test fuel pellet were generated by the pulse irradiation. Grain growth and micro crackings by the pulse irradiation were not obvious.

Acknowledgement

periphery. An interesting point to look at is that if the microscopic cracking was occurred by the pulse irradiation, which could lead an additional fission product gas release in the test. Micrographs taken on the polished samples which experienced the pulse irradiation did not show a clear sign of micro cracking nor grain separation, compared with the micrographs taken on the reference sample which did not experienced a pulse irradiation. The local variation was significantly large and microscopic changes caused by the pulse irradiation was hard to be identified. A quantitative study by porosity measurement etc. is probably needed for further discussion.

8. Conclusions

The following conclusions were obtained through the Test TS-1.

(1) Fabrication of the short test fuel rod from the long commercial rod was successfully performed. The whole test, including assembling, disassembling of the test capsule and PIEs, was conducted without any major troubles. The first test using the refabricated irradiated commercial BWR rod, Test TS-1, provided useful information on fuel performance at a cold start up RIA condition.

(2) The test fuel rod experienced the quick power burst of a maximum enthalpy of 55 cal/g fuel was still intact, showing no residual axial and radial strains. Departure from nucleate boiling did not happened, keeping the cladding surface temperature below 110 °C. No obvious change on the cladding oxidation condition was identified.

(3) Macroscopic radial cracks at the periphery of the test fuel pellet were generated by the pulse irradiation. Grain growth and micro crackings by the pulse irradiation were not obvious.

Acknowledgement

The authers are grateful to the staff members of Hot Engineering Division and Fuel Examination Division of Department of Hot Laboratories for fabricating the test fuel rod with a good quality and also for their excellent pre-pulse examinations. Another set of excellent examinations were conducted for the pulse irradiated fuel rod by members of Research Hot laboratory Division. The authers are grateful to them.

Chemical treatments and isotope measurements for the burnup evaluations were performed by staff members of Analytical Chemistry Laboratory of Department Chemistry. Their careful work is acknowledged.

References

(1) R. W. Miller, "THE EFFECTS OF BURNUP ON FUEL FAILURE 1.Power Burst Test on Low Burnup UO2 Fuel Rods", IN-ITR-113, IDAHO NUCLEAR CORPORATION, July 1970.

(2) R. W. Miller, "THE EFFECTS OF BURNUP ON FUEL FAILURE Power Burst Tests on Fuel Rods with 13,000 and 32,000 MWd/MTU Burnup", ANCR-1280/TID-4500,R63, AEROJET NUCLEAR COMPANY, January 1976.

(3) S. L. Seiffert, Z. R. Martinson and S. F. Fukuda, "Reactivity Initiated Accident Test Series Test RIA 1-1 (Radial Average Fuel Enthalpy of 285 cal/g) Fuel Behavior Report, NUREG/CR-1465/EGG-2040, Idaho National Engineering Laboratory, September 1980.

(4) B. A. Cook, S. K. Fukuda, Z. R. Martinson and P. Bott-Hembree, "Reactivity Initiated Accident Test Series Test RIA 1-2 Fuel Behavior Report", NUREG/CR-1842/EGG-2073, Idaho National Engineering Laboratory, January 1981.

(5) P. E. MacDonald, S. L. Seiffert, Z. R. Martinson, R. K. MacCardell, D. E. Owen and S. K. Fukuda, "Assessment of Light-Water-Reactor Fuel Damage During a Reactivity- Initiated Accident", Nuclear safety, Vol. 21, No. 5, September-October 1980.

(6) S. Saito, T. Inabe T. Fujishiro, et al., "Measurement and Evaluation on Pulsing Characteristics and Experimental Capability", Journal of Nuclear Science and Technology, Vol. 14, No. 3, 1977.

(7) Y. Tsuchie, T. Kodama and Tsuruga Fuel PIE Team, "Post Irradiation Examination of Tsuruga Fuel Using Cladding Tubes Manufactured in Japan", Journal of the Atomic Energy Society of Japan (in Japanese), Vol. 29, No. 3, pp 219-243, 1987.

    The authers are grateful to the staff members of Hot Engineering
Division and Fuel Examination Division of Department of Hot Laboratories for
fabricating the test fuel rod with a good quality and also for their
excellent pre-pulse examinations. Another set of excellent examinations
were conducted for the pulse irradiated fuel rod by members of Research Hot
laboratory Division. The authers are grateful to them.
    Chemical treatments and isotope measurements for the burnup
evaluations were performed by staff members of Analytical Chemistry
Laboratory of Department Chemistry. Their careful work is acknowledged.

References

(1) R. W. Miller, "THE EFFECTS OF BURNUP ON FUEL FAILURE   1.Power Burst
    Test on Low Burnup UO2 Fuel Rods", IN-ITR-113, IDAHO NUCLEAR CORPORATION,
    July 1970.

(2) R. W. Miller, "THE EFFECTS OF BURNUP ON FUEL FAILURE   Power Burst
    Tests on Fuel Rods with 13,000 and 32,000 MWd/MTU Burnup",
    ANCR-1280/TID-4500,R63, AEROJET NUCLEAR COMPANY, January 1976.

(3) S. L. Seiffert, Z. R. Martinson and S. F. Fukuda, "Reactivity Initiated
    Accident Test Series Test RIA 1-1 (Radial Average Fuel Enthalpy of 285 cal/g)
    Fuel Behavior Report, NUREG/CR-1465/EGG-2040, Idaho National Engineering
    Laboratory, September 1980.

(4) B. A. Cook, S. K. Fukuda, Z. R. Martinson and P. Bott-Hembree, "Reactivity
    Initiated Accident Test Series Test RIA 1-2 Fuel Behavior Report",
    NUREG/CR-1842/EGG-2073, Idaho National Engineering Laboratory, January
    1981.

(5) P. E. MacDonald, S. L. Seiffert, Z. R. Martinson, R. K. MacCardell, D. E.
    Owen and S. K. Fukuda, "Assessment of Light-Water-Reactor Fuel Damage
    During a Reactivity- Initiated Accident", Nuclear safety, Vol. 21, No. 5,
    September-October 1980.

(6) S. Saito, T. Inabe T. Fujishiro, et al., "Measurement and Evaluation on
    Pulsing Characteristics and Experimental Capability", Journal of Nuclear
    Science and Technology, Vol. 14, No. 3, 1977.

(7) Y. Tsuchie, T. Kodama and Tsuruga Fuel PIE Team, "Post Irradiation
    Examination of Tsuruga Fuel Using Cladding Tubes Manufactured in Japan",
    Journal of the Atomic Energy Society of Japan (in Japanese), Vol. 29, No. 3,
    pp 219-243, 1987.

(8) Y. Tsuchie and K. Iwamoto, "Post-irradiation Examination (PIE) of Tsuruga Fuel", IAEA Specialists' Meeting on Examination of Fuel Assembly for Water Cooled Power Reactor, IWGFPT/12, pp 221-243, 1981.

(9) Y. Tsuchie and T. Kodama, "Post-irradiation Examination (PIE) of Tsuruga Fuel, Part 2", IAEA Specialists' Meeting on Post- Irradiation Examination and Experience, IWGFPT/22, pp 123-157, IWGFPT/22, 1985.

(10) Y. Tsuchie and K. Iwamoto, "STUDY OF LWR FUEL BEHAVIOR BY CHARACTERIZED TESTS PART II Post-irradiation Examination and Its Related Analysis of Tsuruga Fuel", ANS Topical Meeting on LWR Extended Burnup-Fuel Performance and utilization, pp 2-87 - 2-95, Williamsburg, Virginia, U.S.A., 1982.

(11) K. Yanagisawa et al., "Technical Report: Fabrication of PWR Type Rodlet Fuel", JAERI-M 90-091, May 1990.

Table 1   Characteristics of NSRR

(1) <u>Reactor Type</u>;   Modified TRIGA-ACPR (Annular Core Pulse Reactor)

(2) <u>Reactor Vessel</u>; 3.6^m(wide) × 4.5^m(long) × 9^m(deep) open pool

(3) <u>Fuel</u>;

Fuel type	12 wt% U-ZrH fuel
Fuel enrichment	20 wt% U-235
Clad material	Stainless steel
Fuel diameter	3.56 cm
Clad diameter	3.76 cm O.D.
Length of fuel section	38 cm
Number of fuel rods	157 (including 8 fuel-followered control rods)
Equivalent core diameter	62 cm

(4) <u>Control Rods</u>;

Number	8 (including 2 safety rods)
Type	Fuel followered type
Poison material	Natural B_4C
Rod drive	Rack and pinion drive

(5) <u>Transient Rods</u>;

Number	2 fast transient rods and 1 adjustable transient rod
Type	Air followered type
Poison material	92% enriched B_4C
Rod drive	Fast : Pneumatic
	Adjustable: Rack and pinion & Pneumatic

(6) <u>Core Performance</u>;
a) Steady state operation

Steady state power	300 KW

b) Pulse operation

Max. peak power	21,100 MW
Max. burst energy	117 MW-sec
Max. reactivity insertion	3.4% Δk ($4.67)
Min. period	1.17 msec
Pulse width	4.4 msec (1/2 peak power)
Neutron life time	30 μsec

(7) <u>Experiment Tube</u>;

Inside diameter	22 cm

Table 3 Major characteristics of the BWR test fuel irradiated in Test TS-1

Career	Fuel type	BWR 7x7
	Irradiation Site	TSURUGA-UNIT 1
	Period of Irradiation	1972～1978
	Bundle/rod No.	JAB73/B6
	Bundle ave. Burnup	21.3 GWd/t
	Estimated Rod ave. Burnup	22.0 GWd/t
	Local Burnup	26.0 GWd/t
Test Fuel Rod	Rod No.	01NJJB01 (B6-1)
	Type of Pellet	Dished
	Pellet O.D.	12.37mm (nominal)
	Pellet Length	21.00mm (nominal)
	Fuel Stack Length	126.0mm (nominal)
	^{235}U Enrichment	2.79 % (Initial)
	ditto	0.89[1] % (discharge)
	Fissile Enrichment	1.66[2] % (discharge)
	Cladding O.D.	14.30mm (nominal)
	Cladding Wall Thickness	0.810mm (nominal)
	Pin Pressure	10.82kg/cm² a (at 0°C)
	Gas Composition	Xe/Kr/He(77.9/11.3/10.8)

1) Estimated by ORIGEN-2 code (at 22 GWd/t)
2) Including ^{239}Pu and ^{241}Pu as well as ^{235}U

Table 2 Examples of power histories of NSRR at various operational modes
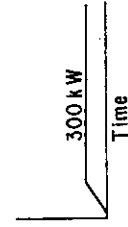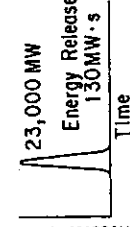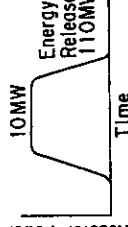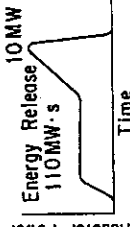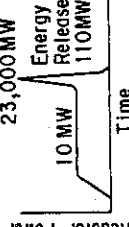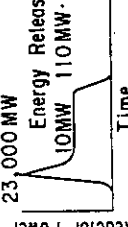
Operation Modes	Operational Limits and Examples of Power History	Research Items
Steady State Operation	300 kW	Decay Heat Simulation etc.
Natural Pulse Operation	23,000 MW, Energy Release 130MW·s	Cold Start-up RIA
Shaped Pulse Operation	10MW, Energy Release 110MW·s	Fuel Relocation Coolability
	10MW, Energy Release 110MW·s	Power Ramping
Combined Pulse Operation	23,000MW, 10 MW, Energy Release 110MW·s	RIA from Rated Power
	23,000 MW, 10MW, Energy Release 110MW·s	High Runout Power

Table 4   Fabrication and chemical composition
of cladding tube[7]

Fuel bundle/cladding	JAB-73
Fabricator	Sumitomo
Final roll	Pilger
Final anneal (°C)	480
Alloy element (ppm)	
Sn	1.48
Fe	0.14
Cr	0.09
Ni	0.06
Fe+Cr+Ni	0.29
Impurities (ppm)	
Al	50
B	<0.5
Cd	<0.5
C	60
Co	<5
Cu	10
Hf	77
Mn	<10
Si	20
Ti	<10
W	<10
U	<3.5
Ca	<5
O	1,275
H	19
N	17

Table 5   Fuel design characteristics[7]

Fuel bundle	
Full length	4,346 mm
Rod array	7×7
Rods/bundle	49
Enrichment	2.50 (bundle average)
〃	2.79, 2.10, 1.80, 1.40
Fuel rod	
Full length	3,964 mm
Effective length	3,657 mm
Pellet material	UO_2, $UO_2+Gd_2O_3$
〃 diameter	12.37±0.03 mm
〃 length	>12.7 mm (non-dished)
〃 〃	21 mm (dished)
〃 density	91~97% T.D.
Clad material	Zircaloy-2
〃 diameter	14.30 mm (O.D.)
〃 thickness	0.81±0.08 mm (=32mil.)
Pellet-clad gap	0.31±0.07 mm (dia.)
Plenum volume	32.6 cm³
Filled gas	He, 1 kg/cm²·a

(Values at room temperature)

Table 7 Condition of data acquisition in Test TS-1

Test No. TS-1   Date October 24, 1989 (14:25)

	Measuring Item	Type of Instruments	ADR Ch.	Gain	Filter	Remarks
1	Cladding Surface #1 Temperature	Pt/Pt-Rh 13%	14	8V/20mV	2kHz	
2	#2	ditto	15	ditto	ditto	
3	#3	ditto	16	ditto	ditto	
4	#4	ditto	17	ditto	ditto	
5	#5	ditto	18	ditto	ditto	
6	#6	ditto	19	ditto	ditto	
7	Water #1 Temperature	CA	20	8V/10mV	ditto	
8	Water #2 Temperature	CA	21	8V/10mV	ditto	
9	Fuel Pressure	Strain Gage	11	18.6 kg/cm²/V		
11	Capsule Pressure	ditto	12	13.89 kg/cm²/V		
12	Capsule Strain	ditto	13	391.62 μst/V		

Table 6 Gas puncturing results of JAB73/B6

		JAB73/B6	Remarks
Gas Volume (cm³)		63.7	± 2cc
Pressure (MPa)		0.99	(at 0°C) ± 10%
Gas Amount (cm³)		609.3	(at 0°C)
Gas Content (%)	H_2	<0.01	
	He	18.13	$110.5cm^3 = 4.93 \times 10^{-3}$ mol
	N_2	<0.01	
	O_2	<0.01	
	Ar	0.31	
	Kr	8.57	$52.2cm^3 = 2.33 \times 10^{-3}$ mol → 17.9% FGR
	Xe	71.9	$438.1cm^3 = 1.96 \times 10^{-2}$ mol → 16.6% FGR
	Xe/Kr	8.69	± 3%

Table 9 Major transient results in Test TS-1

Test No.	TS-1
Core Energy Release (MWs)	72
Reactor Period (ms)	1.6
Inserted Reactivity ($)	3.6
Max. Clad Surface Temperature (°C)	#3 110 / 90 #6 #2 100 / 100 #4 #1 - / 70 #5
Water Temperature (°C)	#1 40 / 40 #2
Max. Pin Pressure Increase (MPa)	—
Max. Pellet Stack Elongation (mm)	—
Max. Cladding Elongation (mm)	—
Failure	No

Table 8 Irradiation conditions for Test TS-1

Item	
Time and Date of Irradiation	14:25, Oct. 24, 1989
Capsule Type	X-II
Capsule Reactivity	-$2.22
Inserted Reactivity	$3.68 (nominal) $3.53 (bank[1]) $3.59 (period[2])
Transient Rod Position TA/TB/T	615/DN/DN
Reactor Period	1.6 ms
NVt #1/#2	74.5/73.5 MWs
Driver Fuel Temperature #1/#2	615/630 °C
Pool Water Temperature	24.6 °C

1) Evaluated from S curve of regulating rod worth (bank operation)
2) Evaluated from reactor period

Table 10 Results of isotope measurement for burnup evaluation

Test TS-1

Isotope		Composition (Atom %)	Concentration (Atoms/g·solution)
U	234	0.0152	5.4141×10^{18}
	235	0.936	
	236	0.352	
	238	98.697	
P u	238	1.475	4.8068×10^{16} $(Pu/U = 8.878 \times 10^{-3})$
	239	59.544	
	240	24.415	
	241	11.076	
	242	3.490	
N d	142	0.282	
	143	20.953	
	144	31.867	
	145	17.079	
	146	16.643	
	148	8.940	2.5460×10^{15}
	150	4.235	
Nd-148/U		4.703×10^{-4}	
Estimated Burnup		2.709 (FIMA%) 26 (GWd/t)	

Table 11 Summary of energy deposition evaluation in Test TS-1

	Pronpt (Max. Enthalpy)	1s (Nominal)	∞ (Total)
Iserted Reactivity ($)	3.68		
Reactor Energy Release (MWs)	66	72.4	83
Number of fissions (fissions/g·fuel)[1]	8.27×10^{12}	9.05×10^{12}	1.04×10^{13}
Fission Energy (MeV/fission)	175.3	176.4	186.4
Energy Deposition (cal/g·fuel)[1]	55.4	61.1	74.1

1) Initial amount of UO_2 is defined as the weight of fuel.

Table 12 Summary of test conditions and
results in Test TS-1

Test No.	TS-1
Local Burnup (GWd/t)	26
Fill gas	Xe+Kr+He (1. 1MPa)
Energy Deposition (cal/g·fuel)	61
Max. Fuel Enthalpy (cal/g·fuel)	55
Core Energy Release (MWs) Reactor Period (ms) Inserted Reactivity ($)	72 1. 6 3. 6
Max. Clad Surface Temperature (℃)	#3 110 ／ 90 #6 #2 100 ／ 100 #4 #1 — ／ 70 #5
Water Temperature (℃)	#1 40 ／ 40 #2
Max. Pin Pressure Increase (MPa)	—
Max. Pellet Stack Elongation (mm)	—
Max. Cladding Elongation (mm)	—
Failure	No

Fig. 1 NSRR core configuration

offset loading tube

⇧

B (SS Linear, FC) ⊗
A (SS Log, FC) ⊗
F (High Power, ⊗
Linear, CIC)

⊗ E (High Power Log, FC)
⊗ C1 (Safety, CIC)
⊗ D1 (Pulse, μFC)

Experiment
tube

Transient rod (3)

Instrumented Fuel (3)

Safety rod (2)

Regulating rod (6)

D2 (Pulse, μFC) ⊗   ⊗ C2 (Safety, CIC)
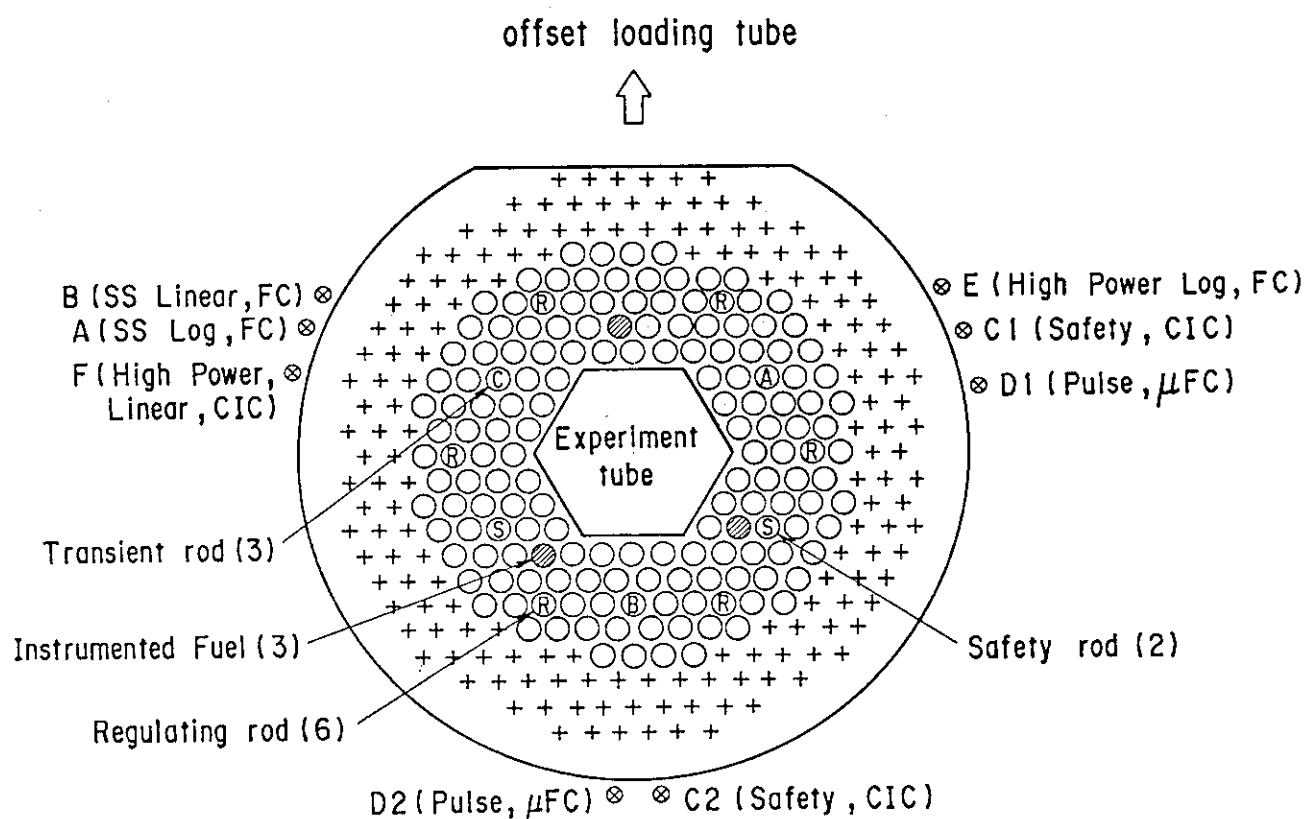
SS   : Steady state operation (≦ 300 KW)

High Power : High power operation during shaped pulse and combined
              pulse operations (≦ 10 MW)

A, B, C   : Transient Rod A, B, C

Fig. 2 NSRR rod arrangement
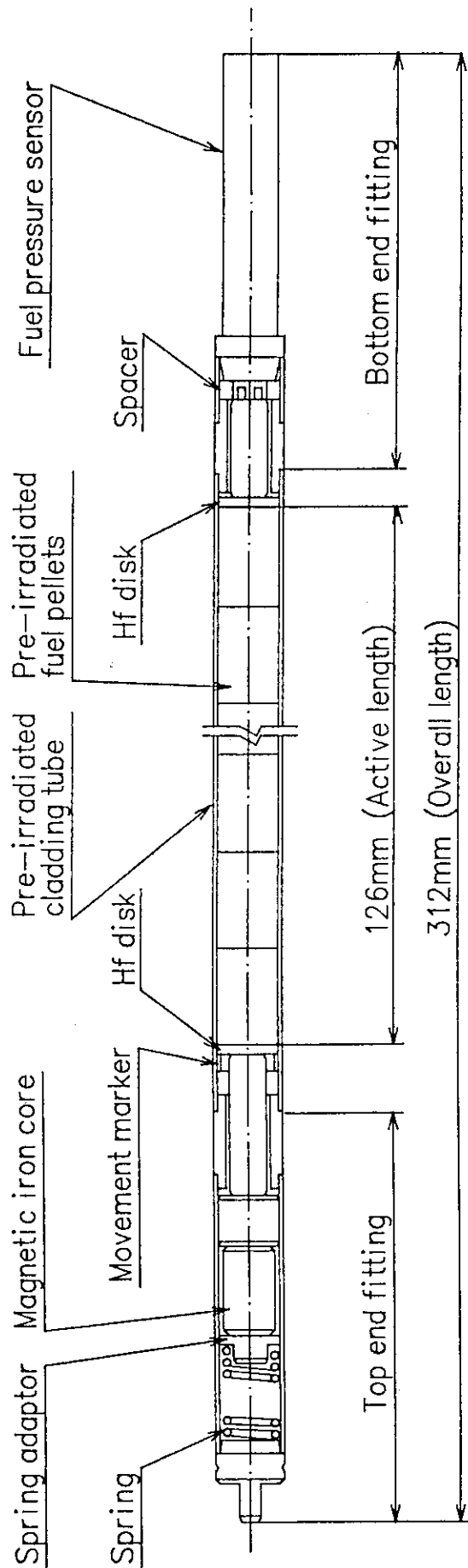
Fig. 3 Structure of the test fuel rod
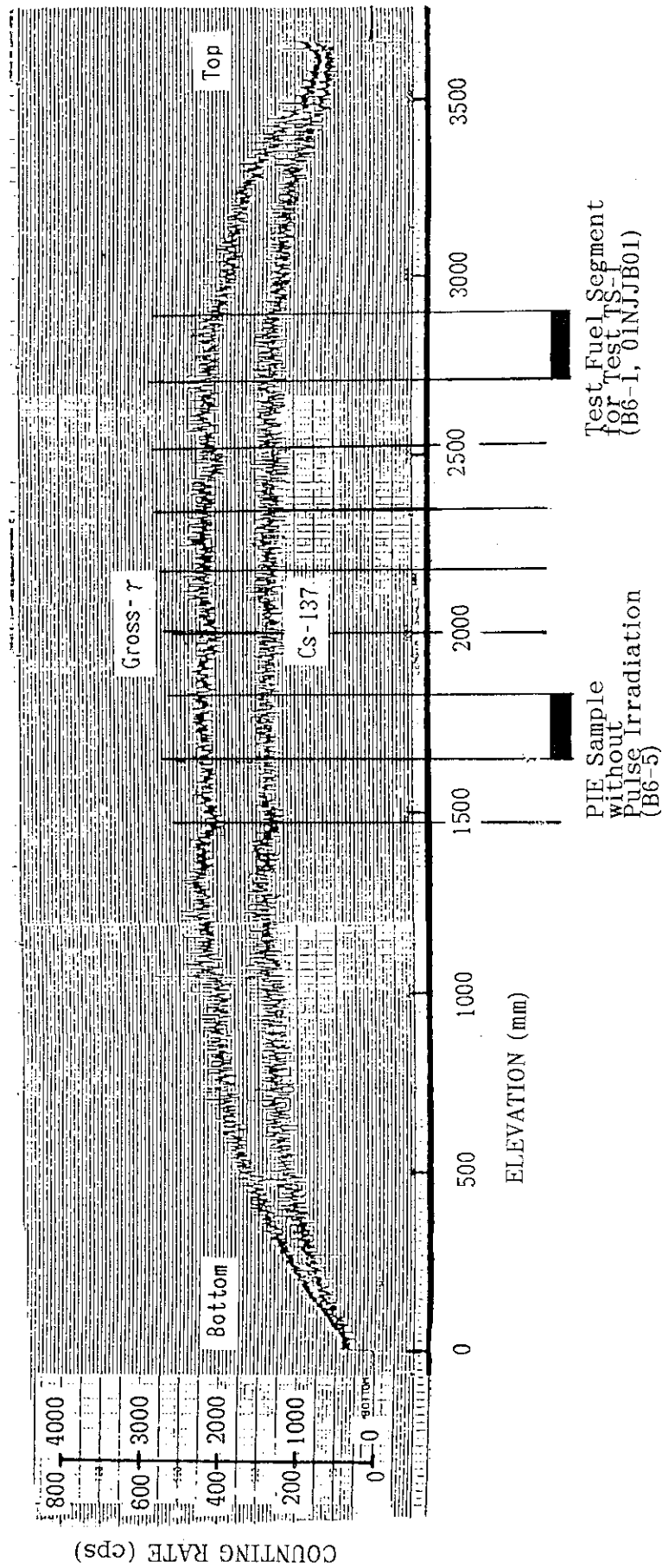
Fig. 4   γ scanning profile of BWR fuel and segmented location
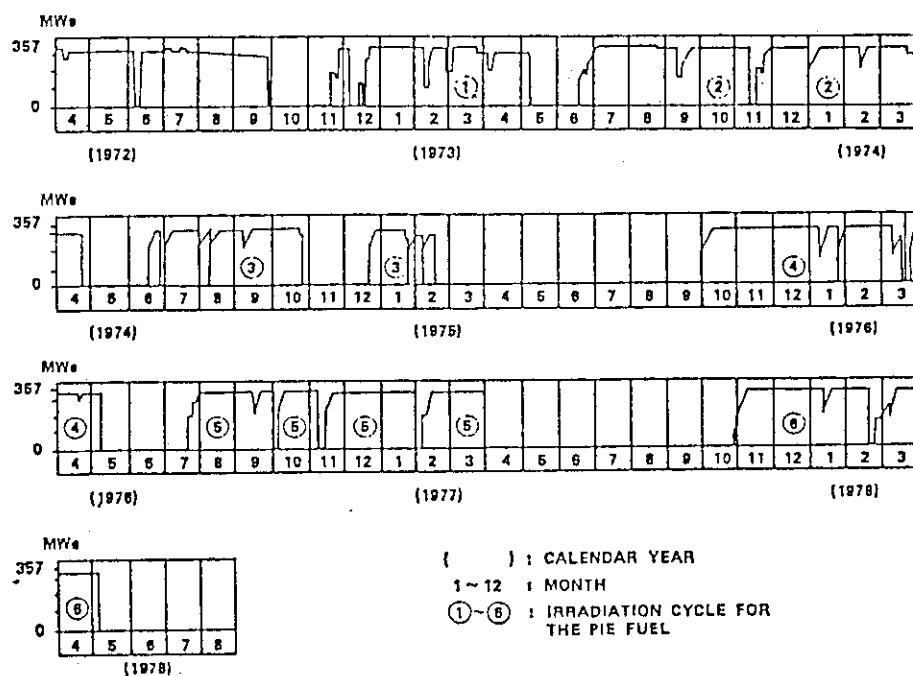
Fig. 5 Operational history of Tsuruga reactor[7]

("; F4 ROD IS ADDED AS CAT-I FOR JAB-73.)

○ : CATEGORY-I (NDT + DT) : 5 RODS/B'DL

△ : " -II (NDT ONLY): 18 " / "

⊕ : TIE ROD

⊕' : SEGMENTED ROD

○d : DISHED PELLET ROD
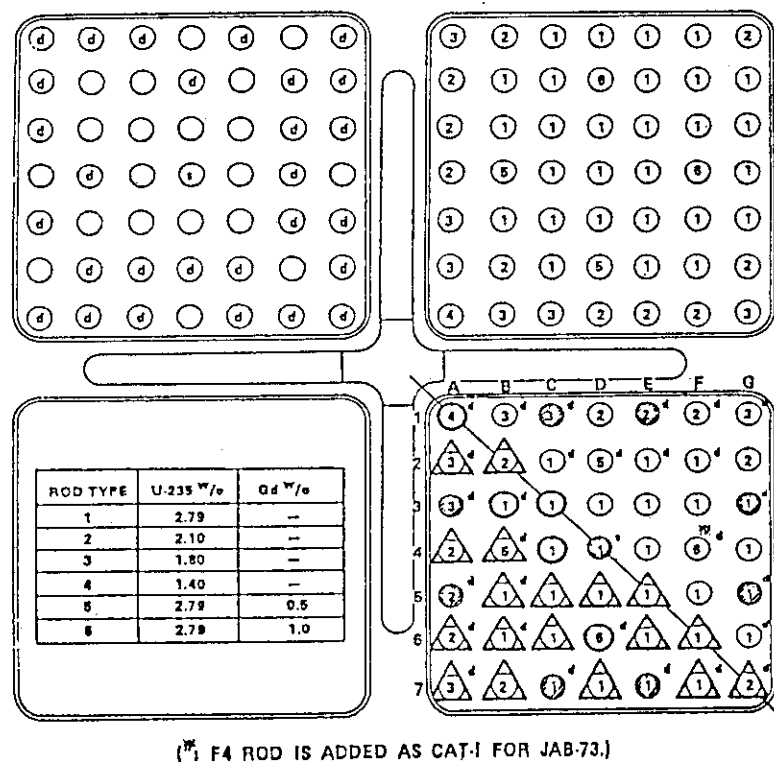
Fig. 6 Fuel rod positions within bundle[7]
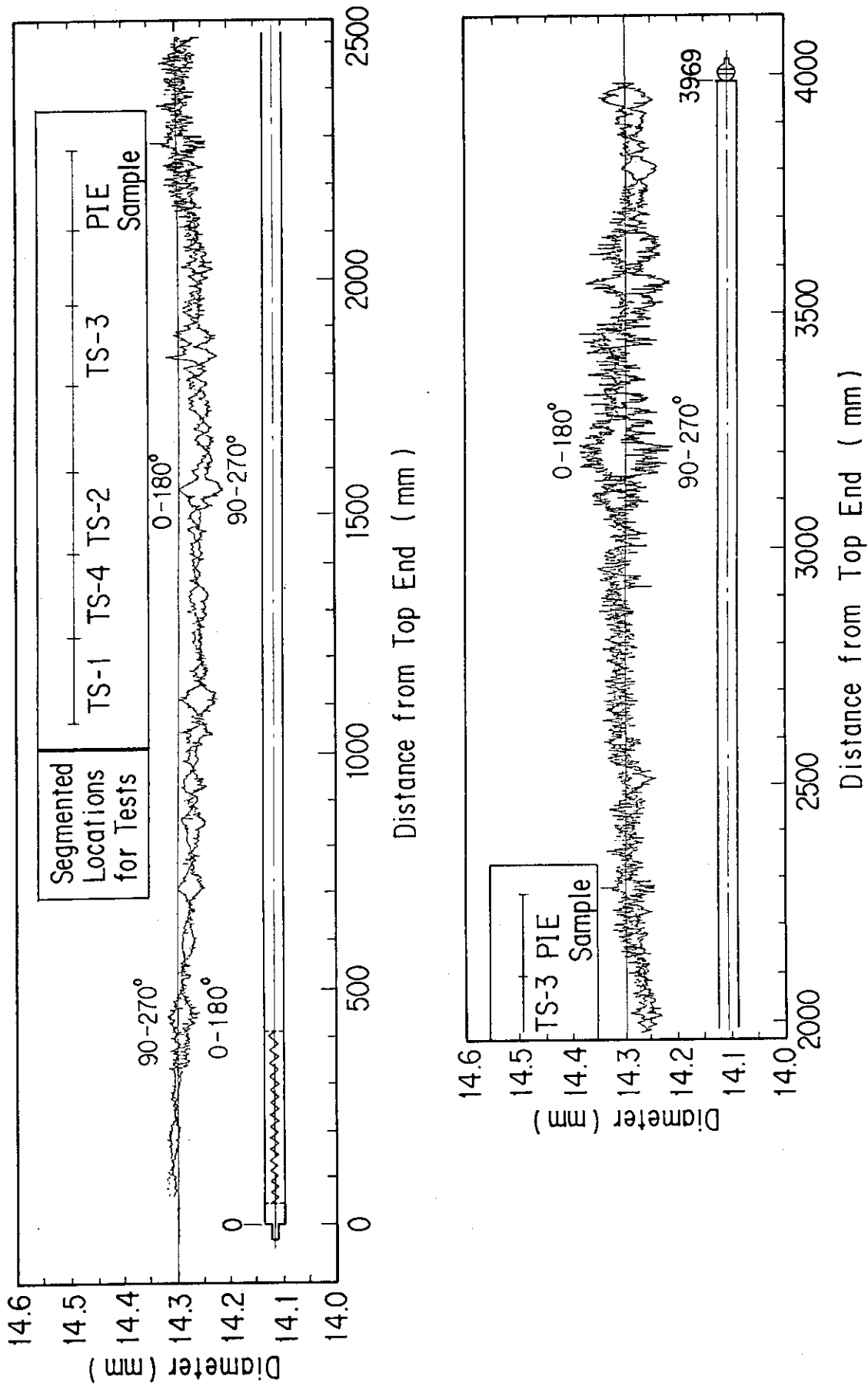
Fig. 7 Diameter profile of long sized commercial rod JAB73/B6 for TS test series
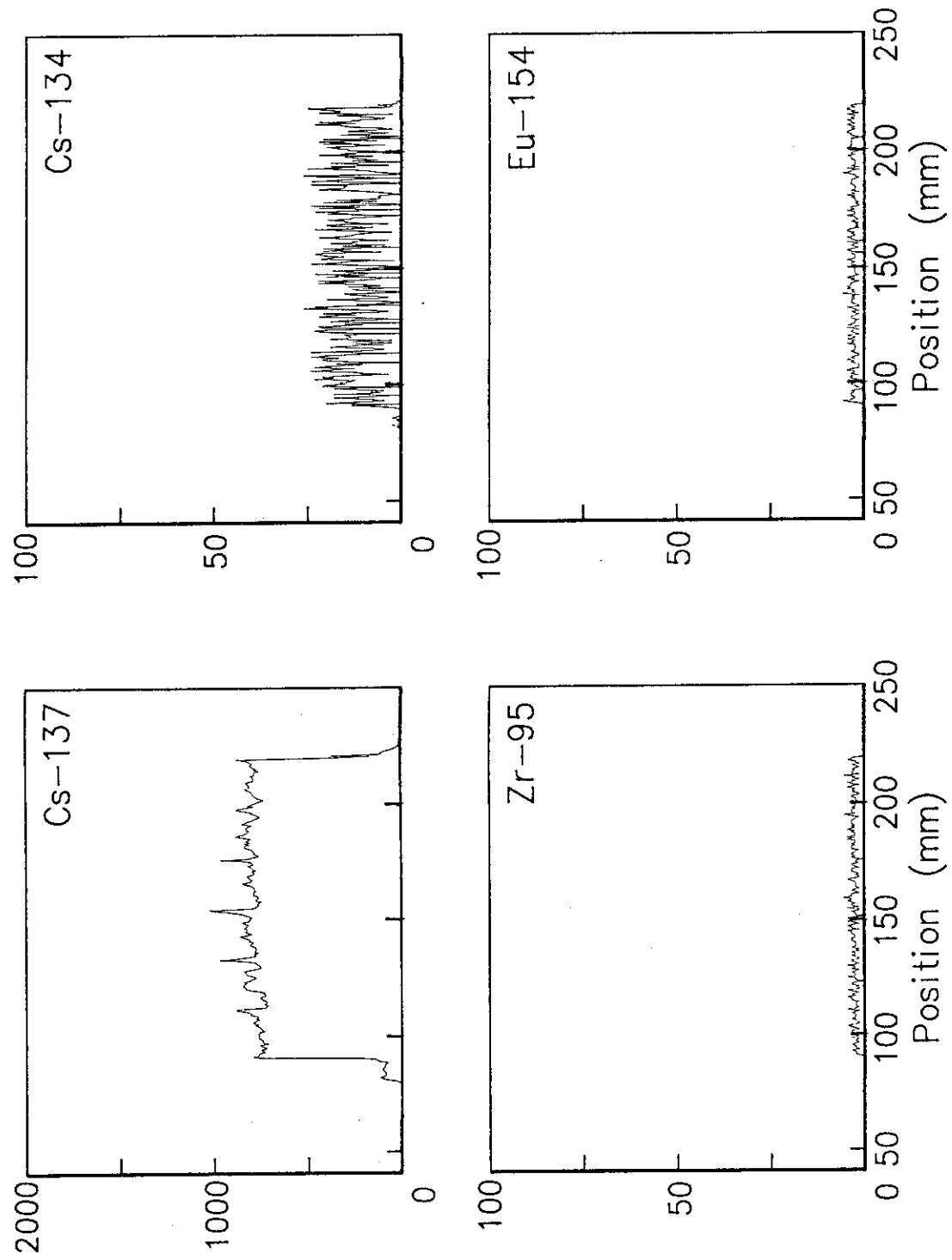
Fig. 8 γ-scanning profiles of test fuel rod provided for Test TS-1 (Before pulse irradiation)
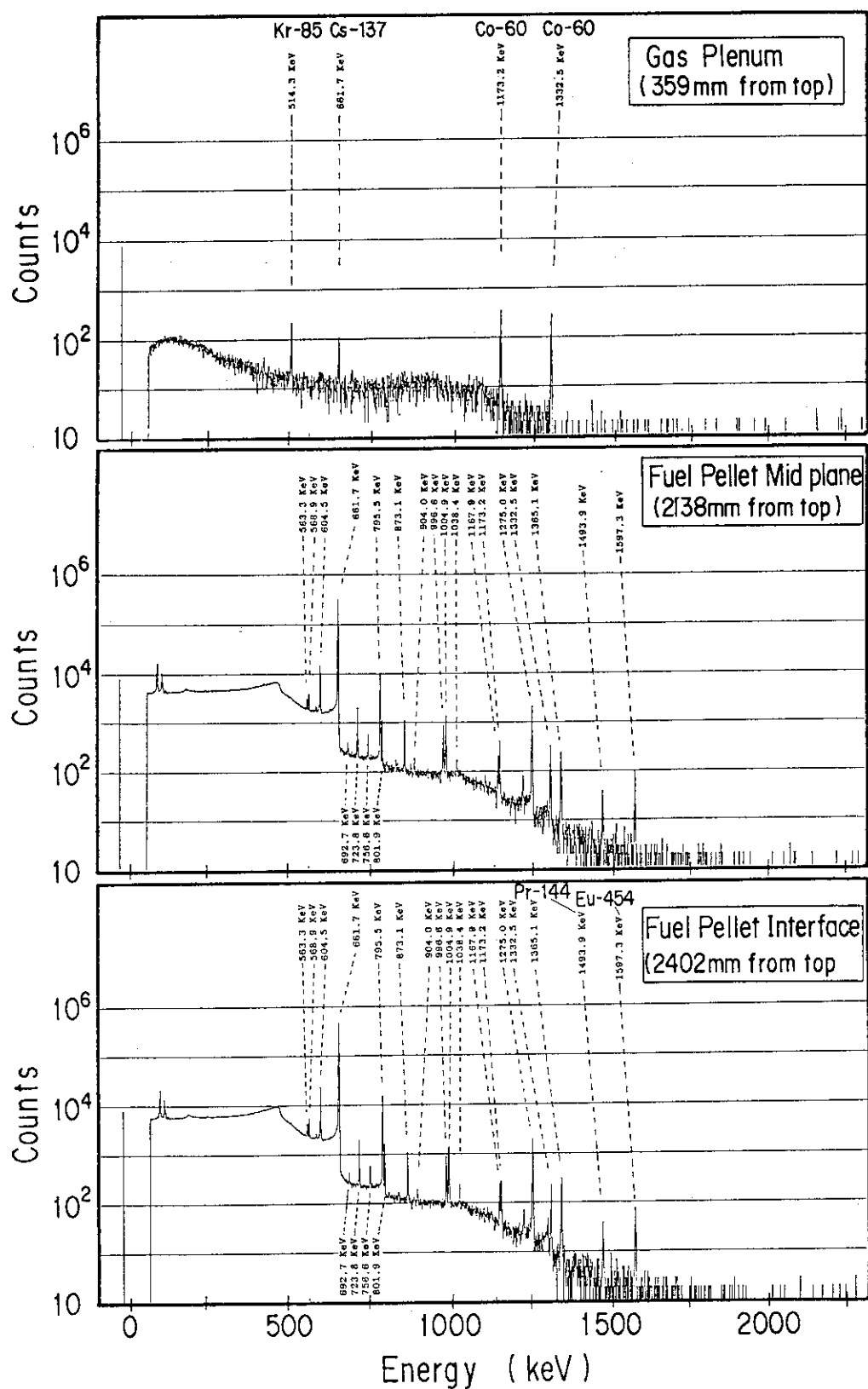
Fig. 9 γ spectra at typical locations of commercial rod JAB73/B6 for TS test series
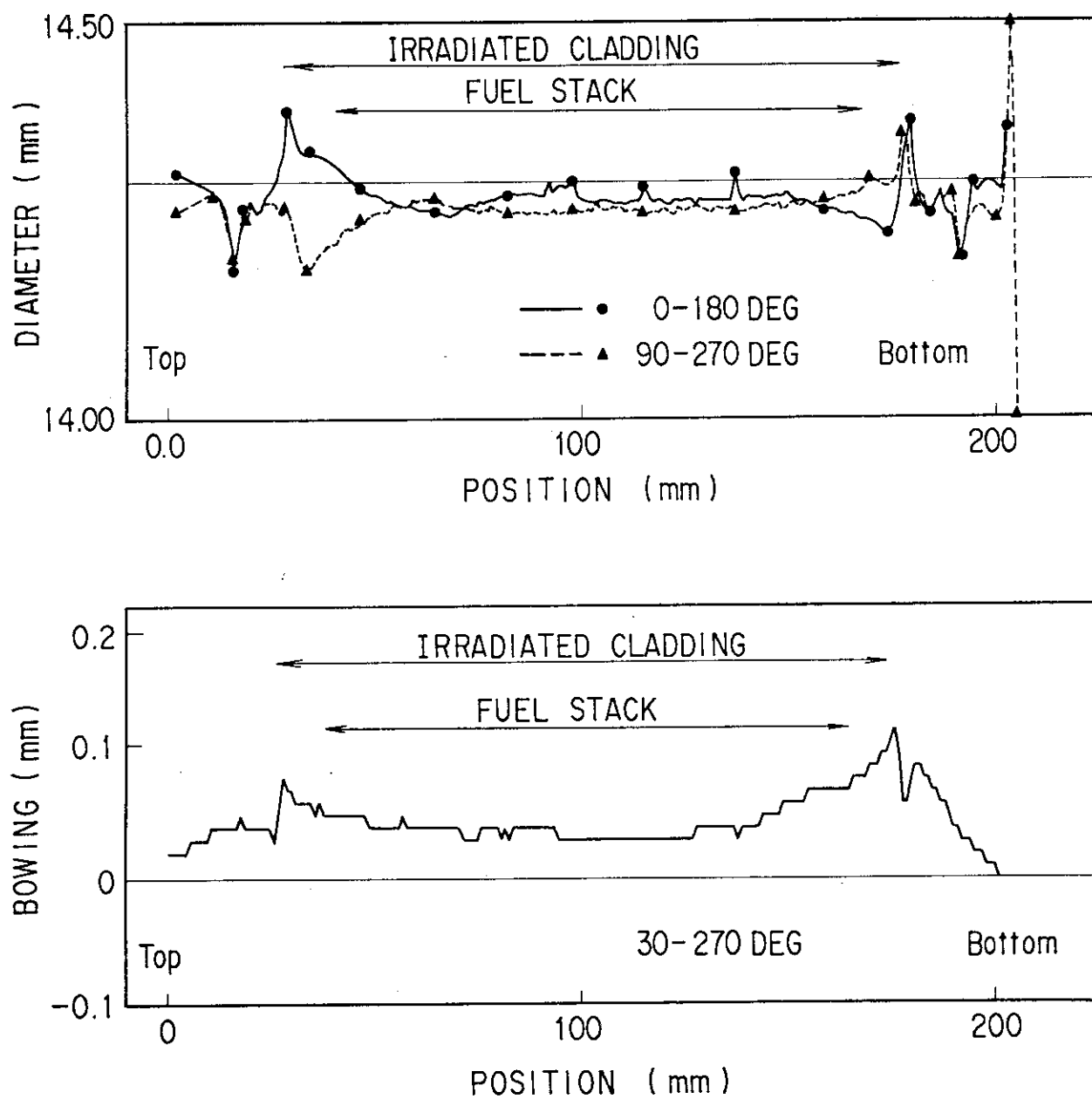
Fig. 10   Diameter and bowing profiles of test fuel rod
provided for Test TS-1 (Before pulse irradiation)

Test TS-1			Frequency (kHz)	Gain (db)	Phase (°)
		X_1, Y_1	64	−20	155
Rod No.	01NJJB01 (B6−1)	X_2, Y_2	512	−20	340
Before pulse irradiation			$X_3=X_1+X_2,\ Y_3=Y_1+Y_2$		

Marker(1 mm/pitch)

X_1 component

Y_1 component

X_2 component

Y_2 component

Axial Position(mm)

X_3 component

Y_3 component

Marker(100mm/pitch)

IRRADIATED CLADDING

FUEL STACK
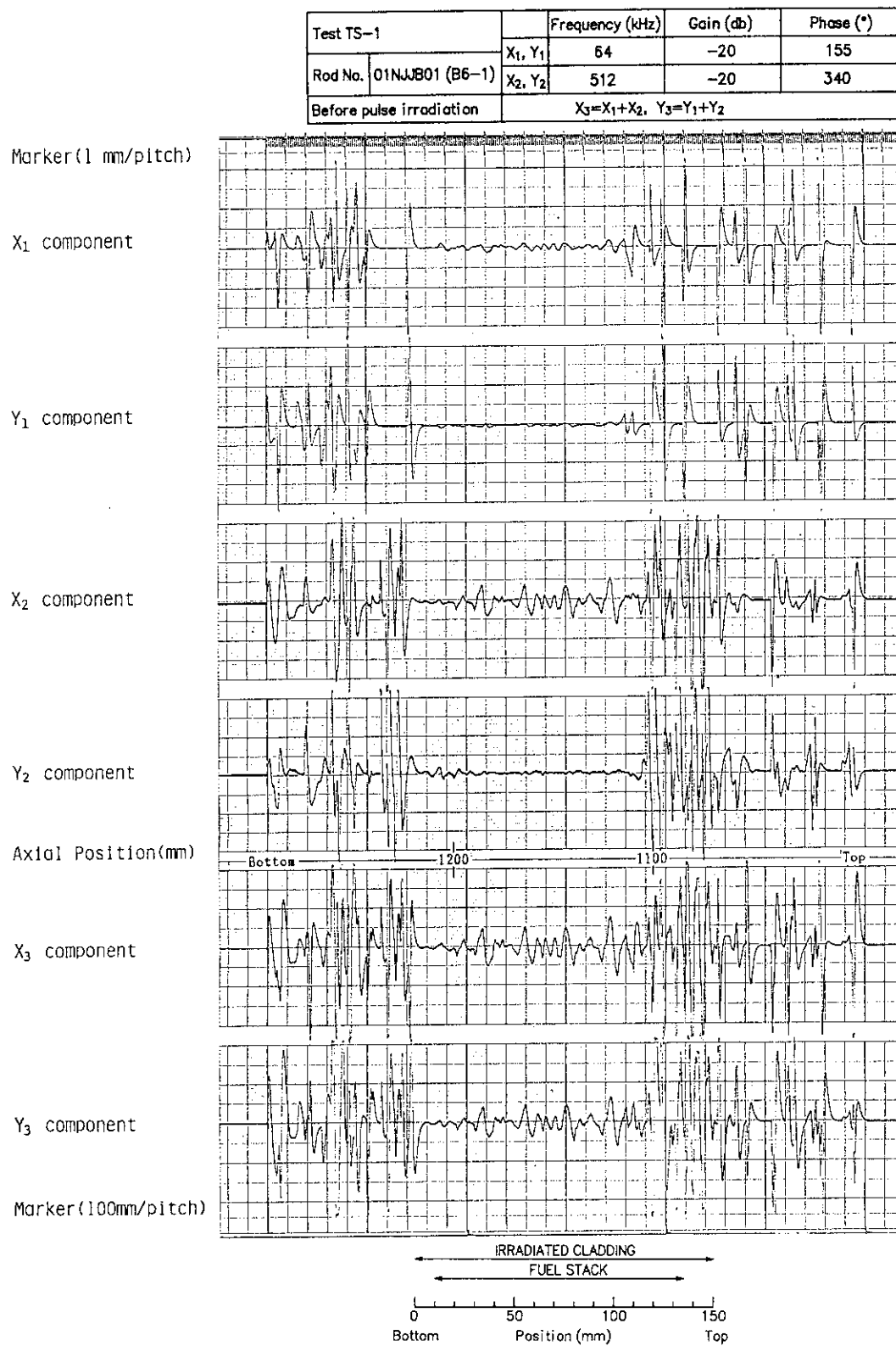
Fig. 11 Eddy current test results of test fuel rod provided
for Test TS-1 (Before pulse irradiation)
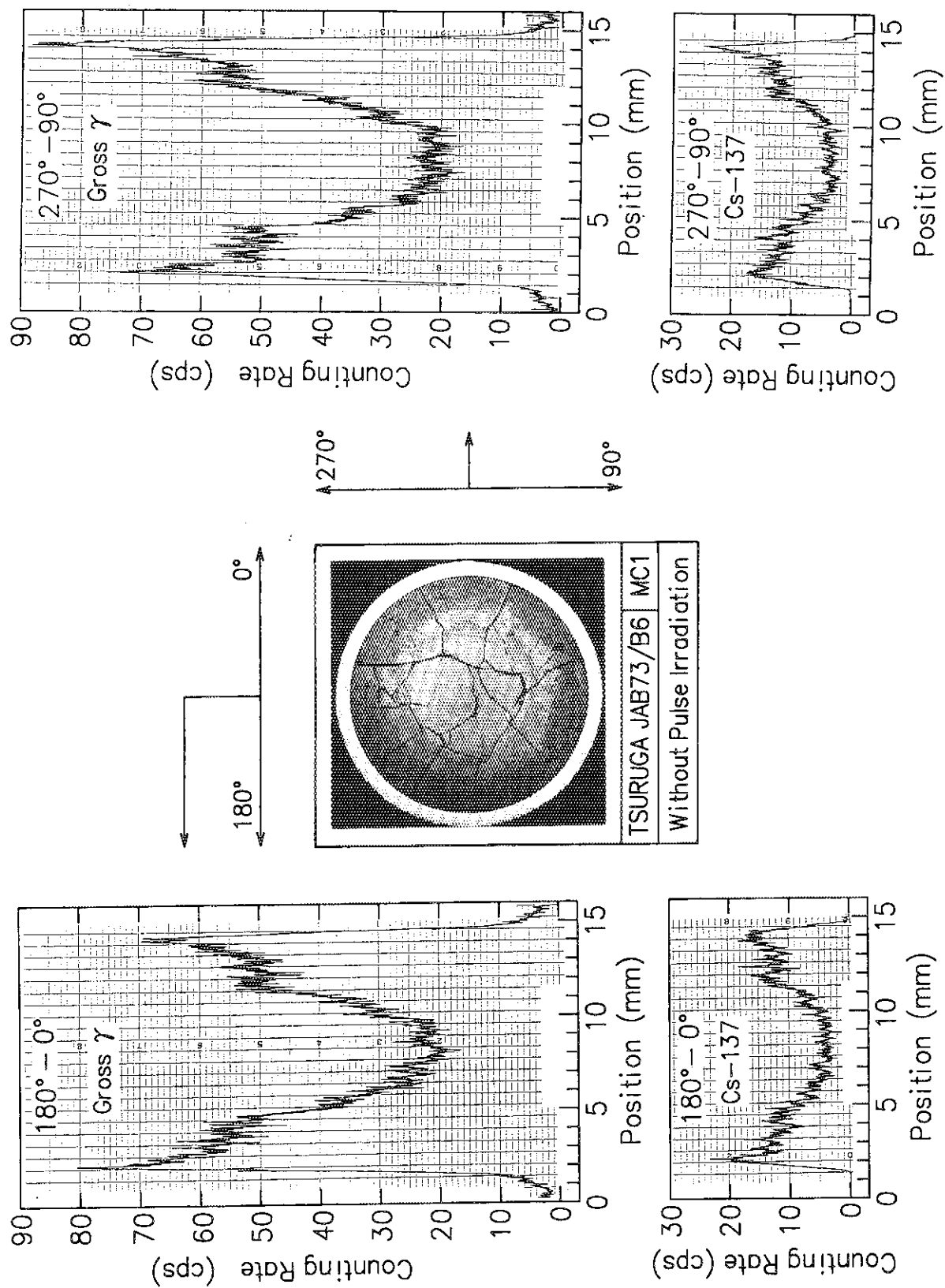
Fig. 12 Micro γ-scanning profiles of commercial rod JAB73/B6 for TS test series

Capsule cap

Hanger fixing bolt

Top closure
(Outer capsule)

Gas discharge valve
(Inner capsule)

Hanger rod

Water level
(Inner capsule)

Test fuel

Capsule body
(Inner capsule)

Capsule body
(Outer capsule)

Gas discharge valve
(Outer capsule)

Flange bolt
(Outer capsule)

Instrumentation plug
(Outer capsule)

Water level
(Outer capsule)

Instrumentation plug
(Inner capsule)

Flange bolt
(Inner capsule)

Top closure
(Inner capsule)

150

1250

1100

Unit (mm)

φ 200

Fig. 13   Schematic configuration of type X-II atmospheric pressure
capsule for pre-irradiated fuel rod test

Fig. 14　Instrumentation for BWR fuel rod tests (TS series)
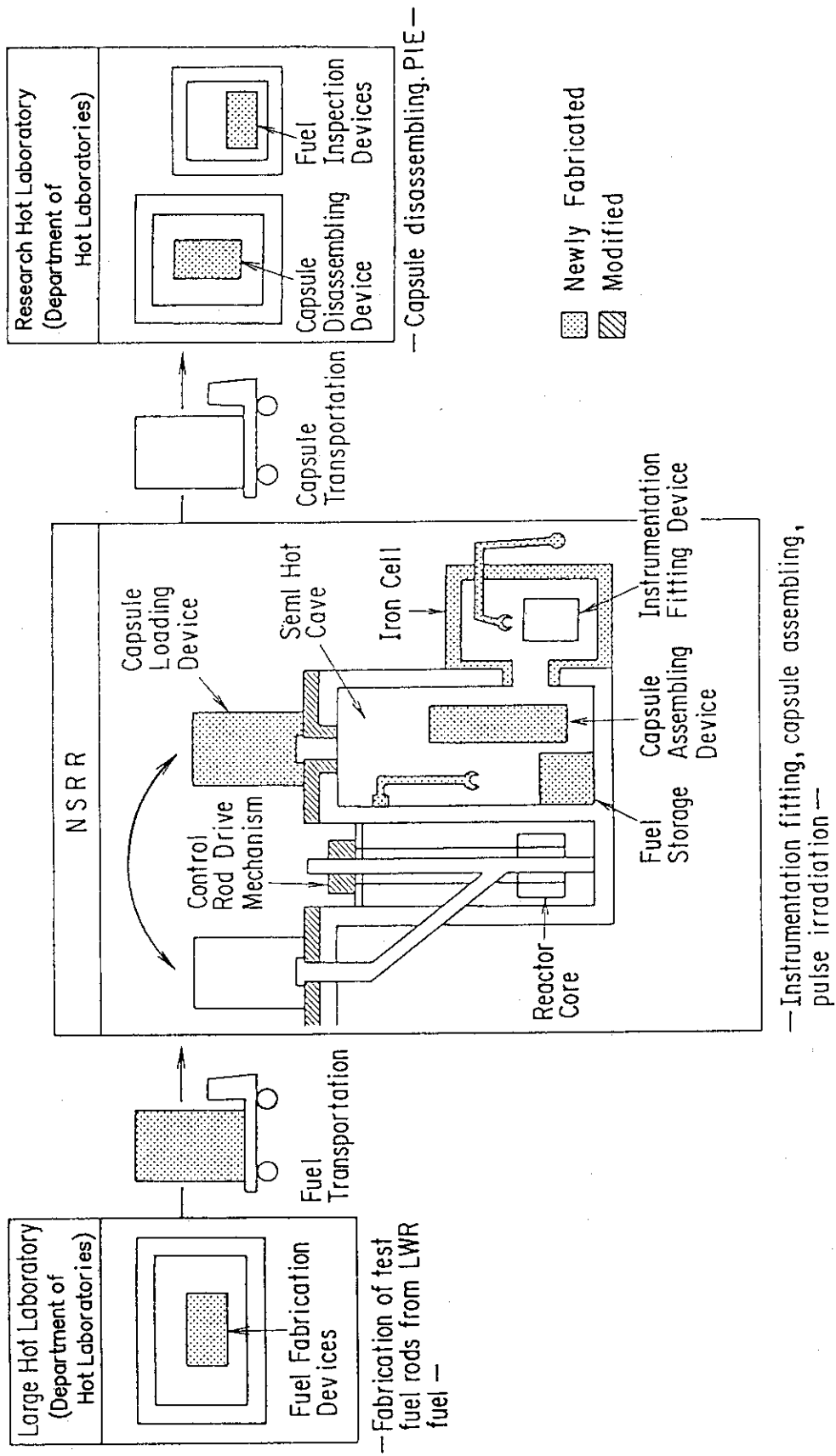
Fig. 15 Outline of the handling procedure for TS test series
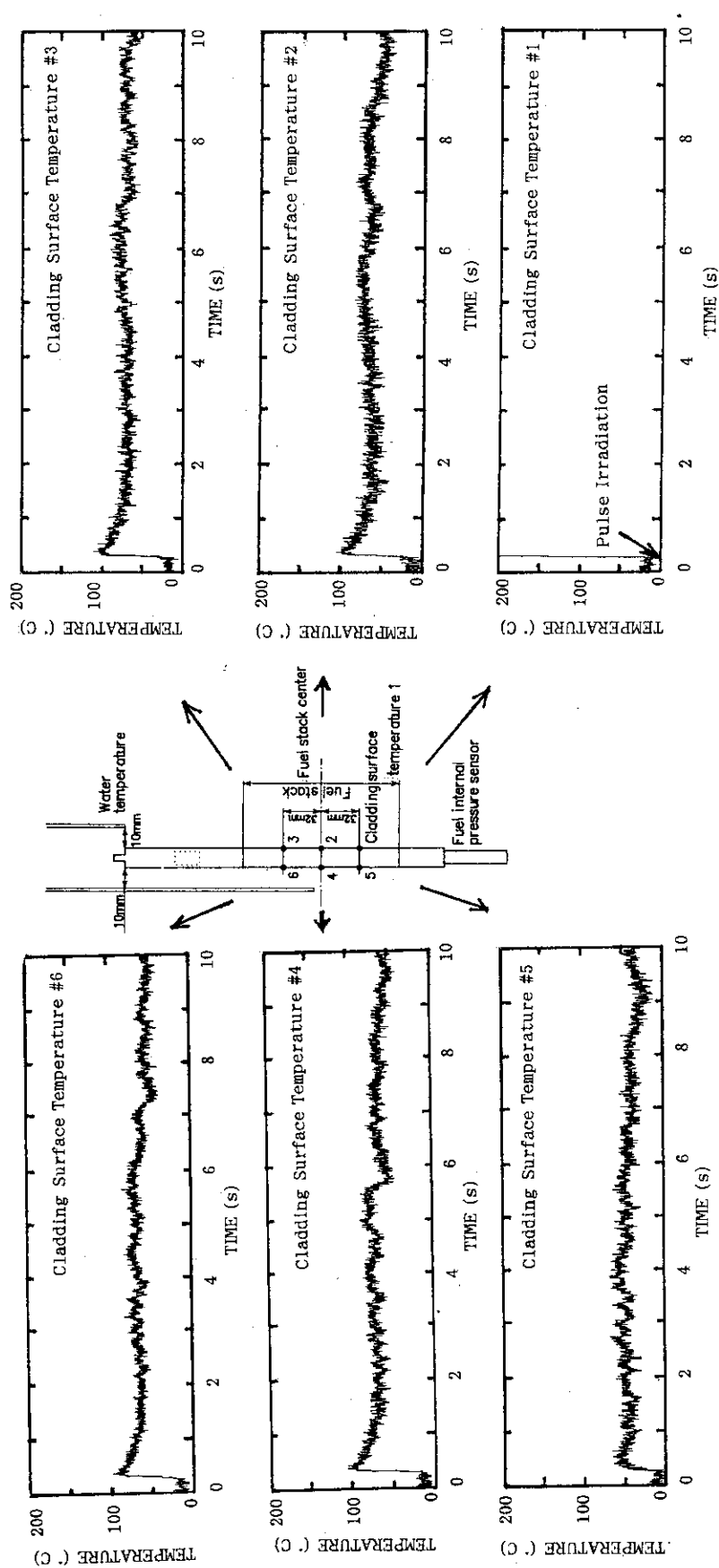
Fig. 16 Cladding surface temperature histories observed in Test TS-1 (0-10s)
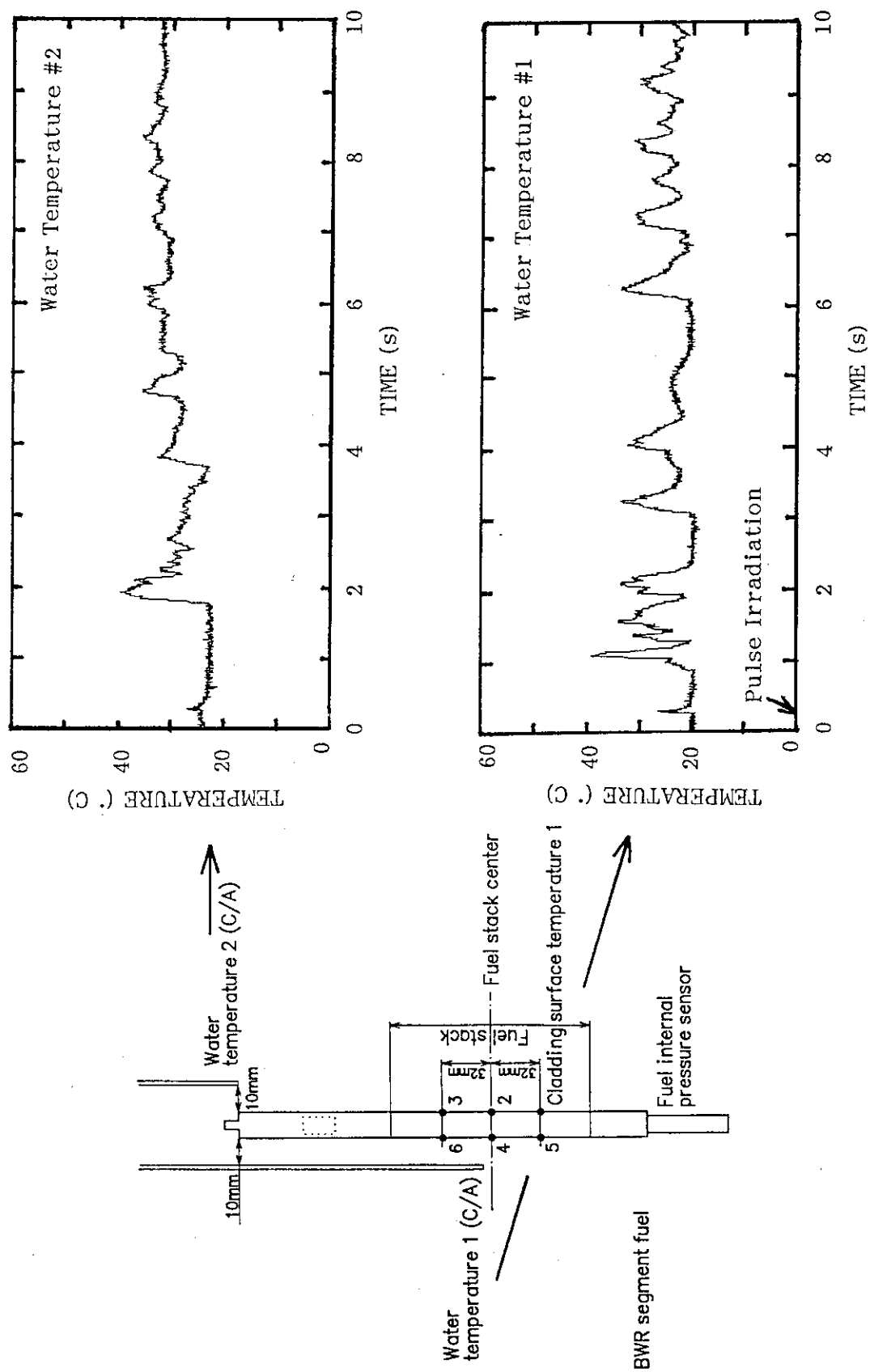
Fig. 17 Water temperature histories observed in Test TS-1 (0-10s)
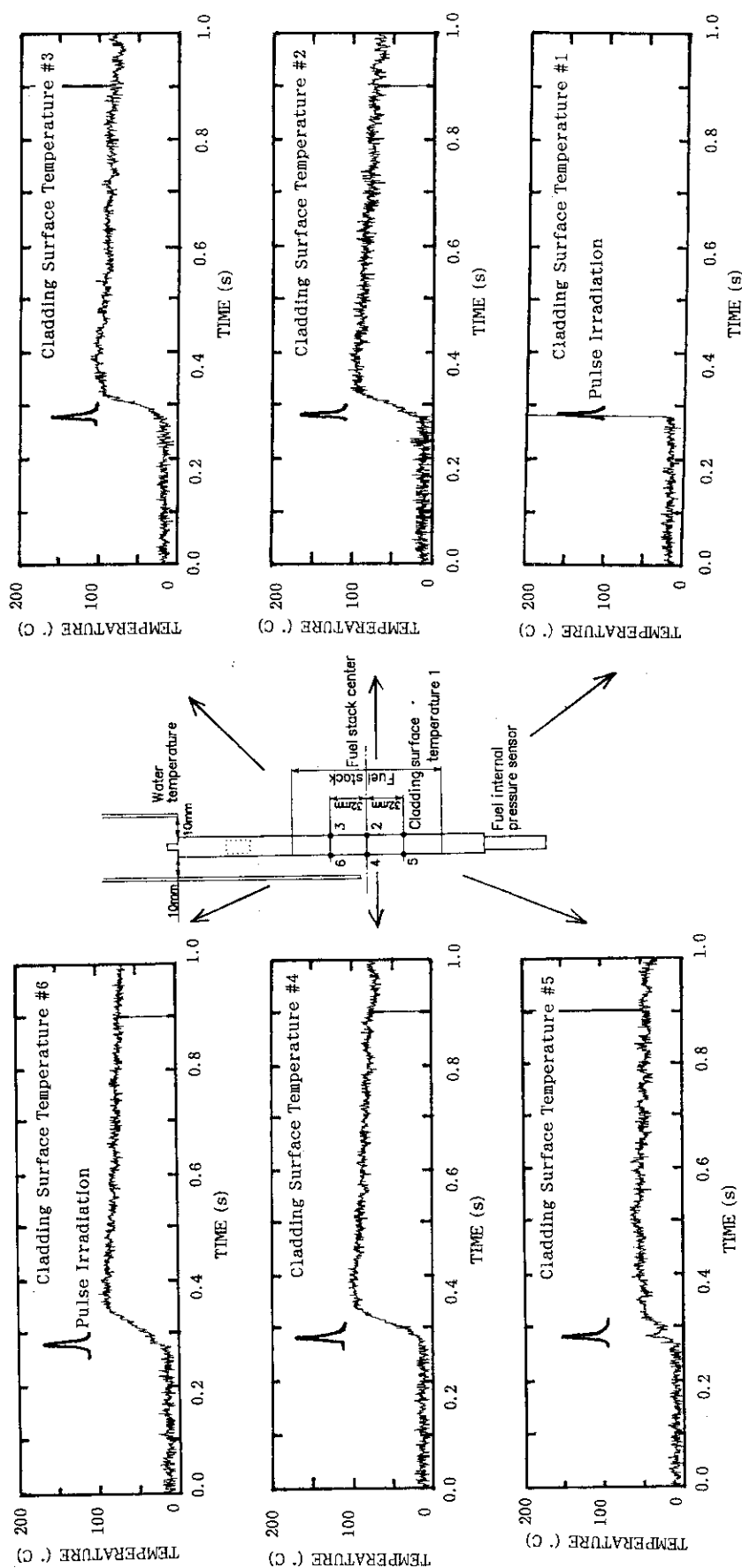
Fig. 18 Cladding surface temperature histories observed in Test TS-1 (0-1s)
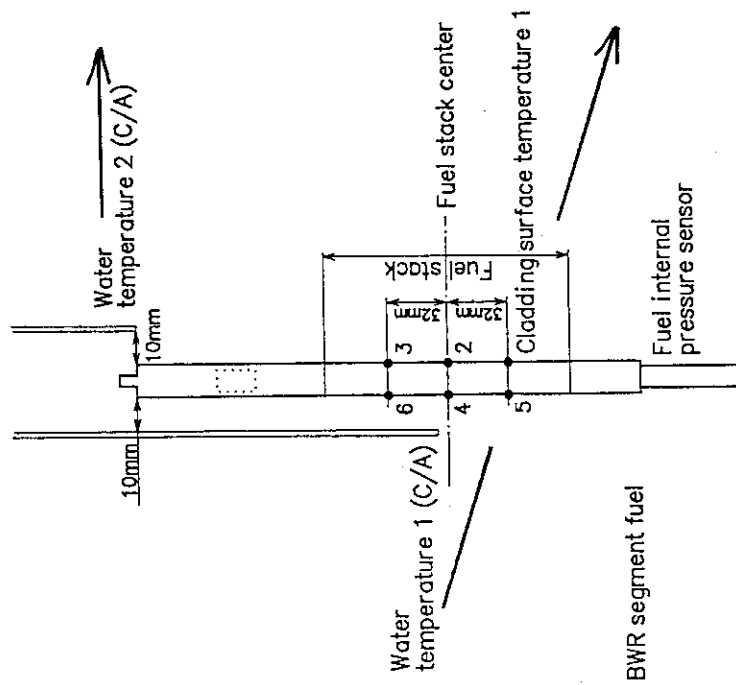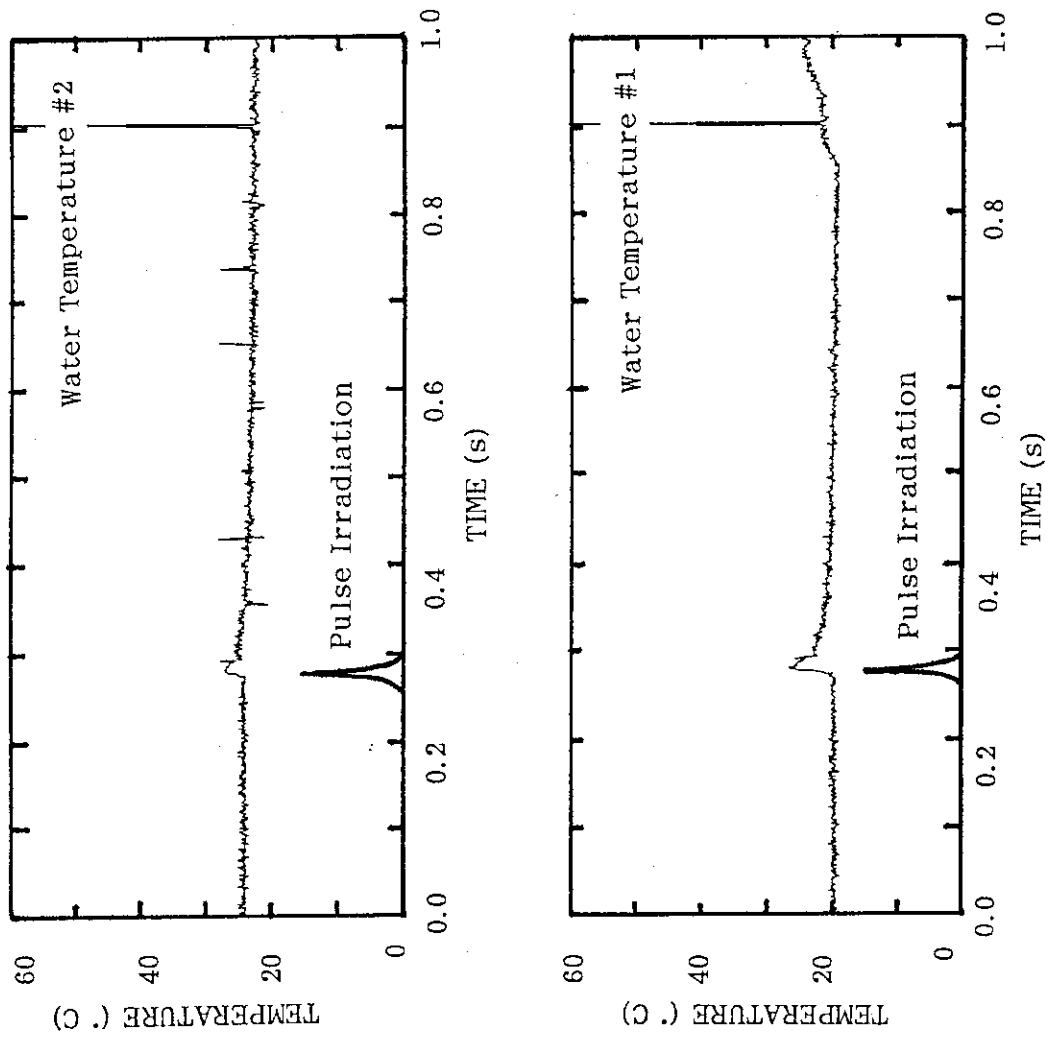
Fig. 19 Water temperature histories observed in Test TS-1 (0-1s)
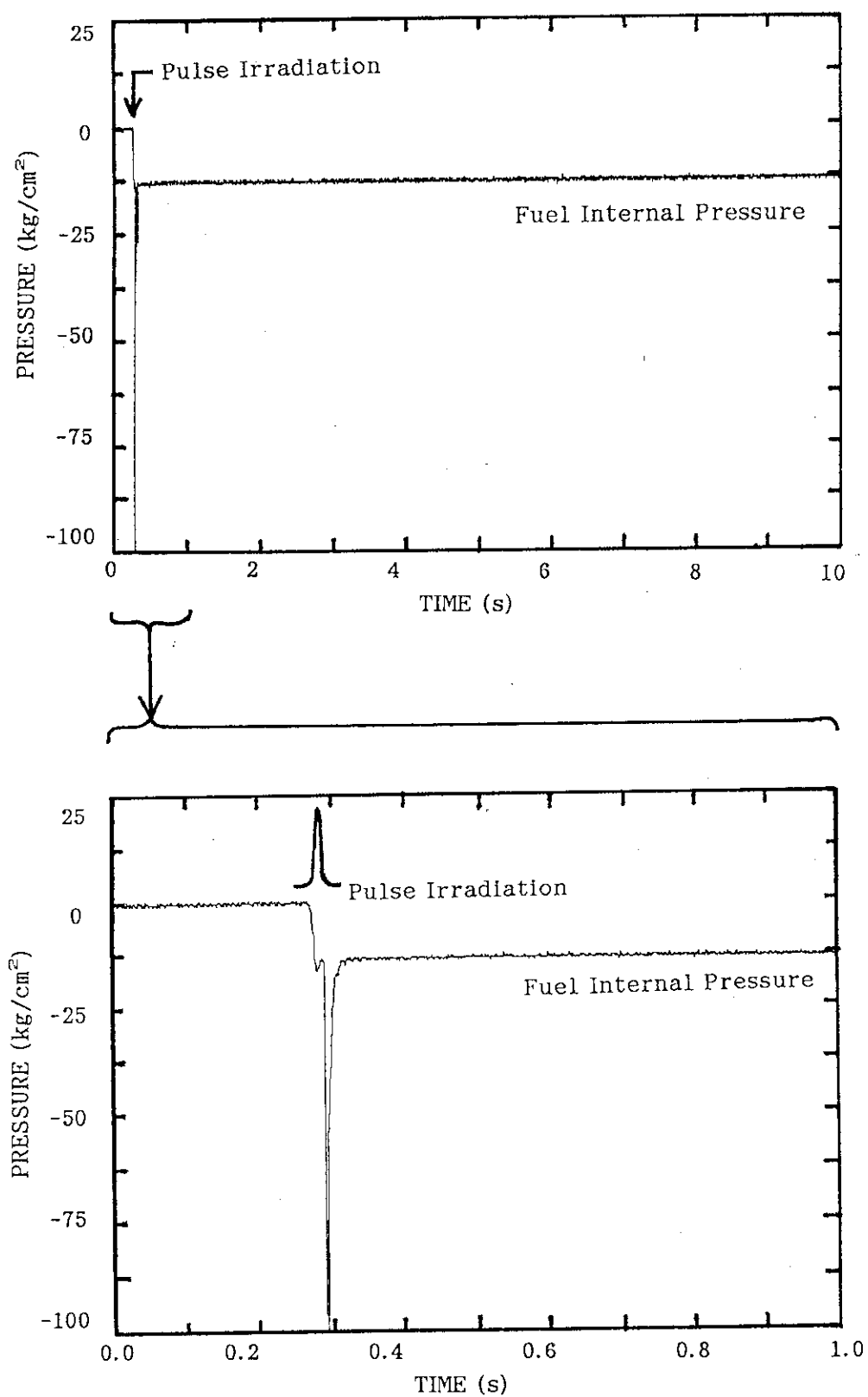
Fig. 20 Fuel internal pressure sensor response during pulse irradiation
in Test TS-1

Test Fuel Rod
  |
Resin Injection ∠——— Resin
  |
Cutting(Diamond Cutter) thickness : ~2mm (UO₂ : ~1g)
  |
Weighing Sample with Cladding and Resin
  |
Dissolution ∠——— 8 Mol Nitric Acid
  |
Filtration ———≥ Weighing Cladding, Resin and Insoluble Residue
  |
Sampling (4M HNO₃ Solution, ~ 1 mg UO₂)
  |

Sample for Chemical Separation	
Sample A	Sample B
Sample for Isotopic Composition Measurement of U,Pu and Nd	Sample for Burnup Measurement Determination of U,Pu and Nd by Isotopic Dilution Method(IDM)

¹⁵⁰Nd, ²³³U, ²⁴²Pu Spiked for IDM

Fig. 21 Flow of solution preparation

Sample A and B

─── Ba-133(44 Bq) for Determination of Ba
Chemical Yield

Anion Exchange, Hydrochrolic Acid System

FP   Zr   Pu   Np   U

(Mass Spec.)   (Mass Spec.)

Anion Exchange, Methanol-Nitric Acid System

Cs,Sr,Y   Ba,Eu   Cm   Am   Nd

(Mass Spec.)

Cation Exchage, Nitric Acid System

Ba   Eu

Burnup

Gamma-ray Spectrometry ─────(Chemical Yield)─ ─ ─ ─

Determination of Ba-133 and Ba-140 Contents ───┬──U Contents

(Ba-140 Fission Yield) ────

cal/g UO₂   Number of Fission/g UO₂

Fig. 22 Flow of Ba separation and fuel energy deposition evaluation
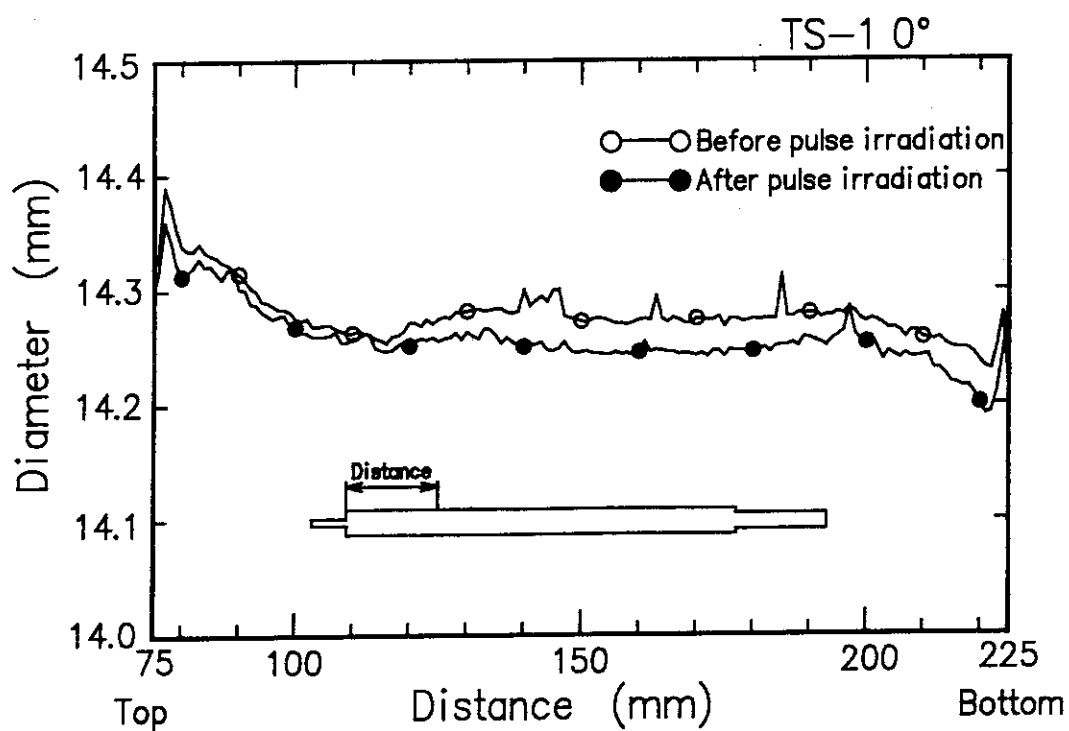
Fig. 23 Diameter profiles of test fuel rod in Test TS-1
before and after pulse irradiation (0-180°)
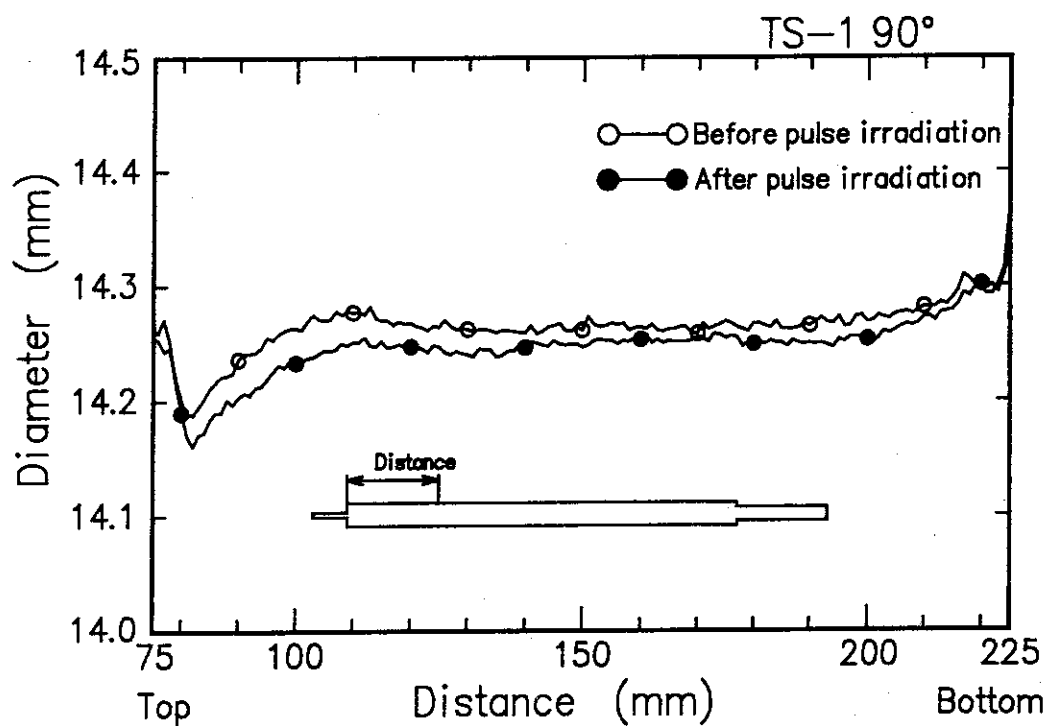
Fig. 24 Diameter profiles of test fuel rod in Test TS-1
before and after pulse irradiation (90-270°)

BOTTOM

TOP

Test TS-1

After Pulse Irradiation

Rod No. 01NJJB01

Nov. 14 , 1989
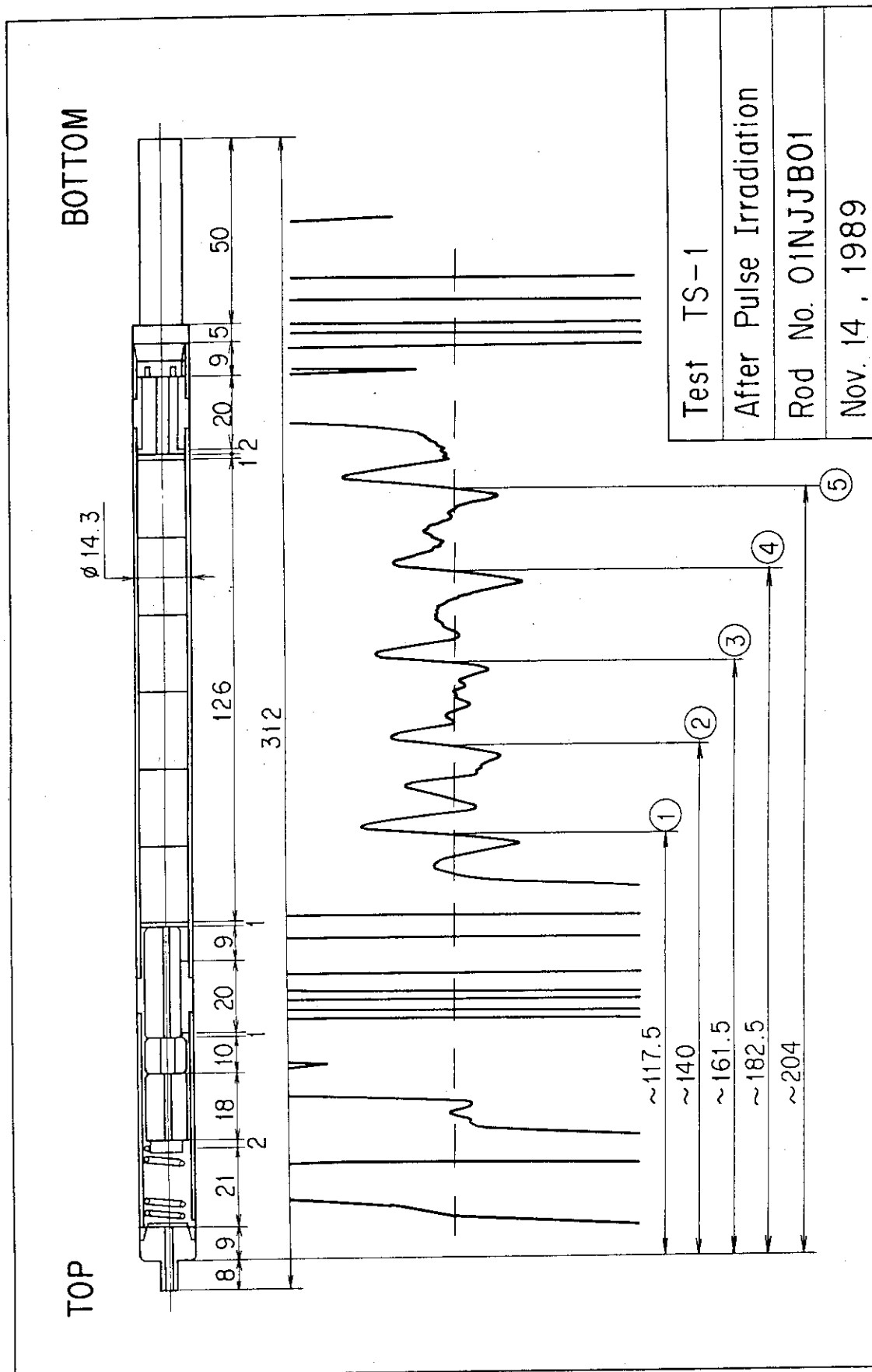
Fig. 25 Eddy current test result of pulse irradiated test fuel rod in Test TS-1
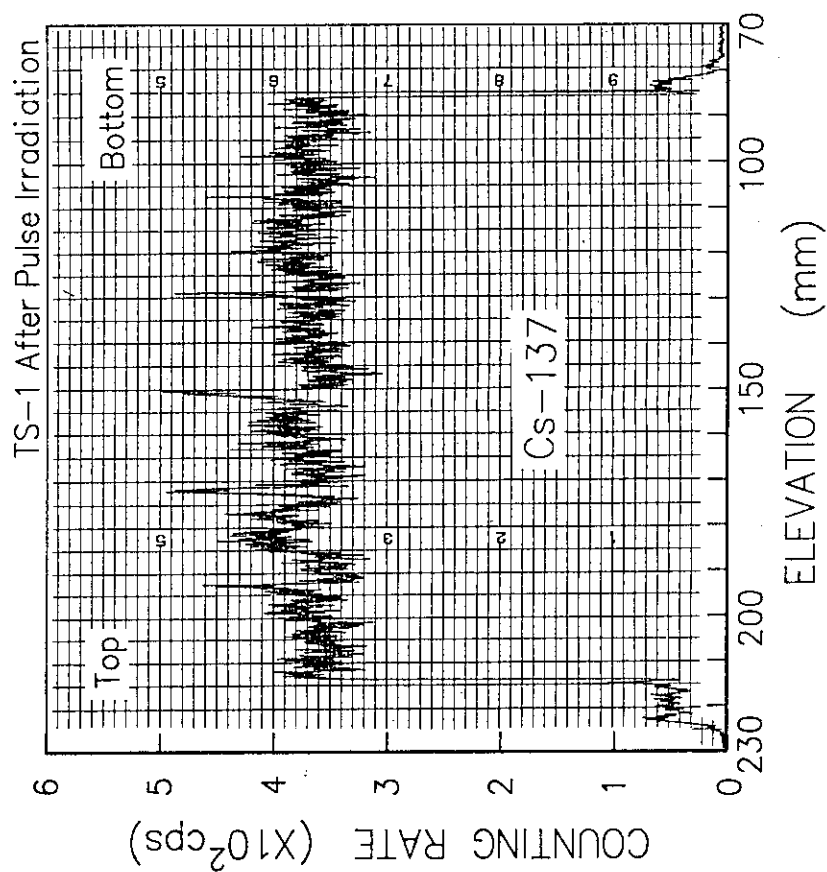
Fig. 27 γ-scanning profile of test fuel rod pulse
irradiated in Test TS-1 (Cs-137)

Fig. 26 γ-scanning profile of test fuel rod pulse
irradiated in Test TS-1 (Gross γ)

Fig. 28 γ-spectra at typical locations of pulse irradiated
test fuel rod in Test TS-1
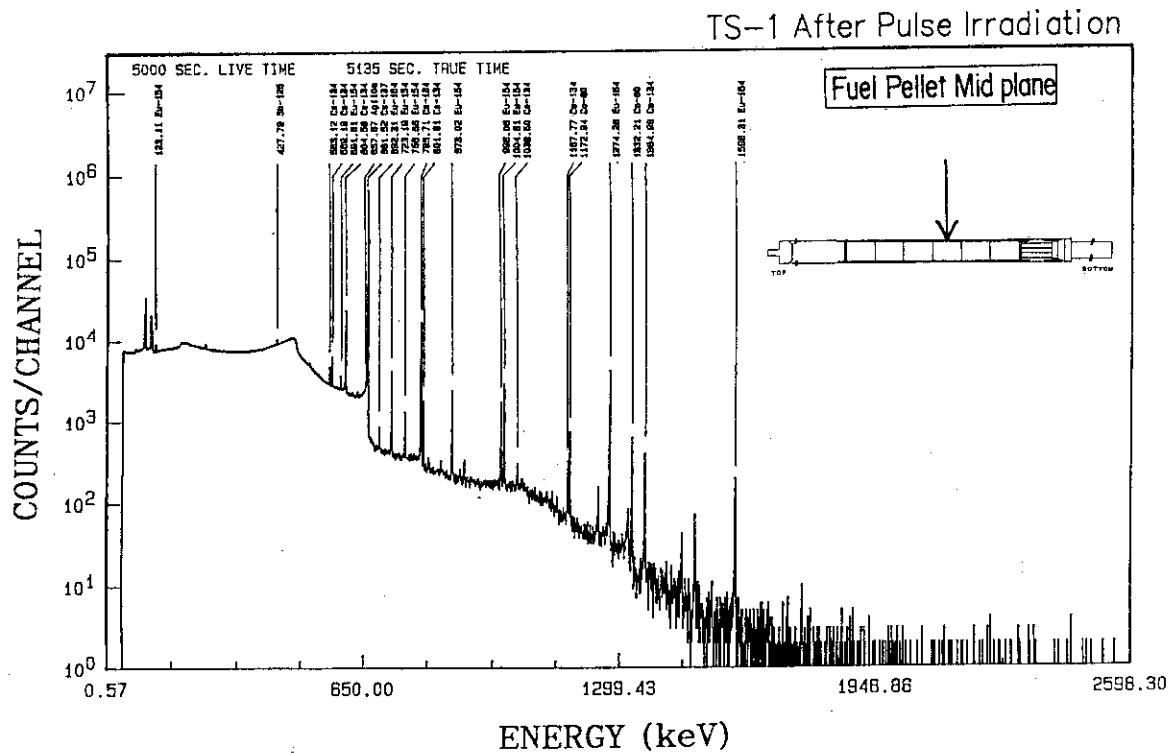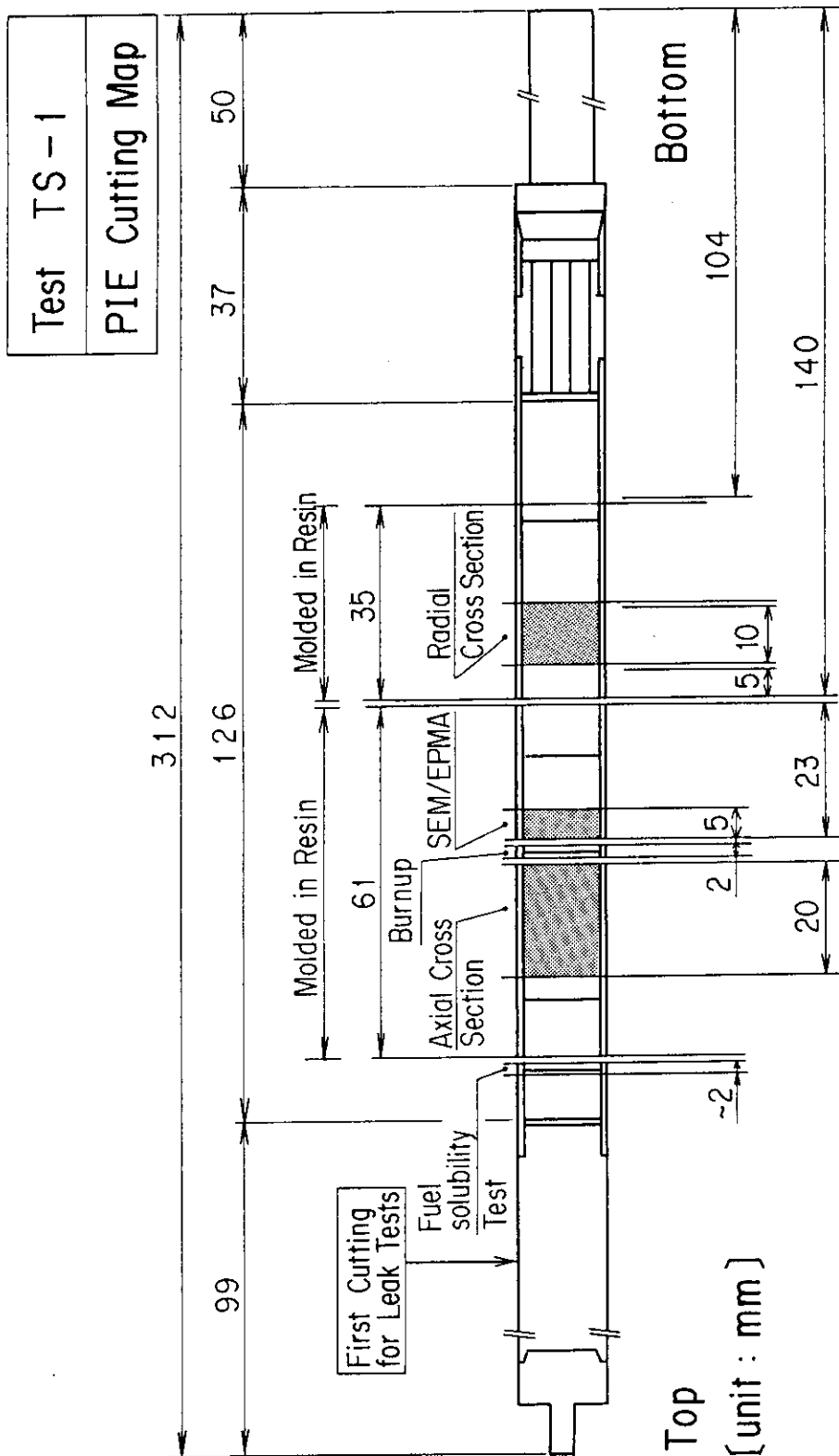
Fig. 29 Cutting map of samples for destructive tests in Test TS-1
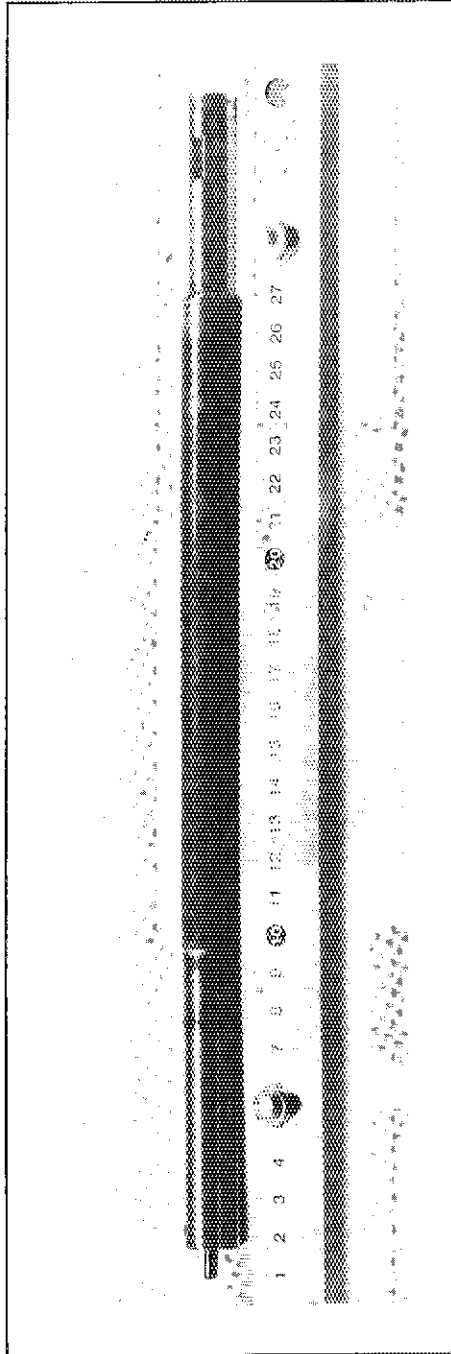
Photo. 1 Appearance of test fuel rod provided for Test TS-1
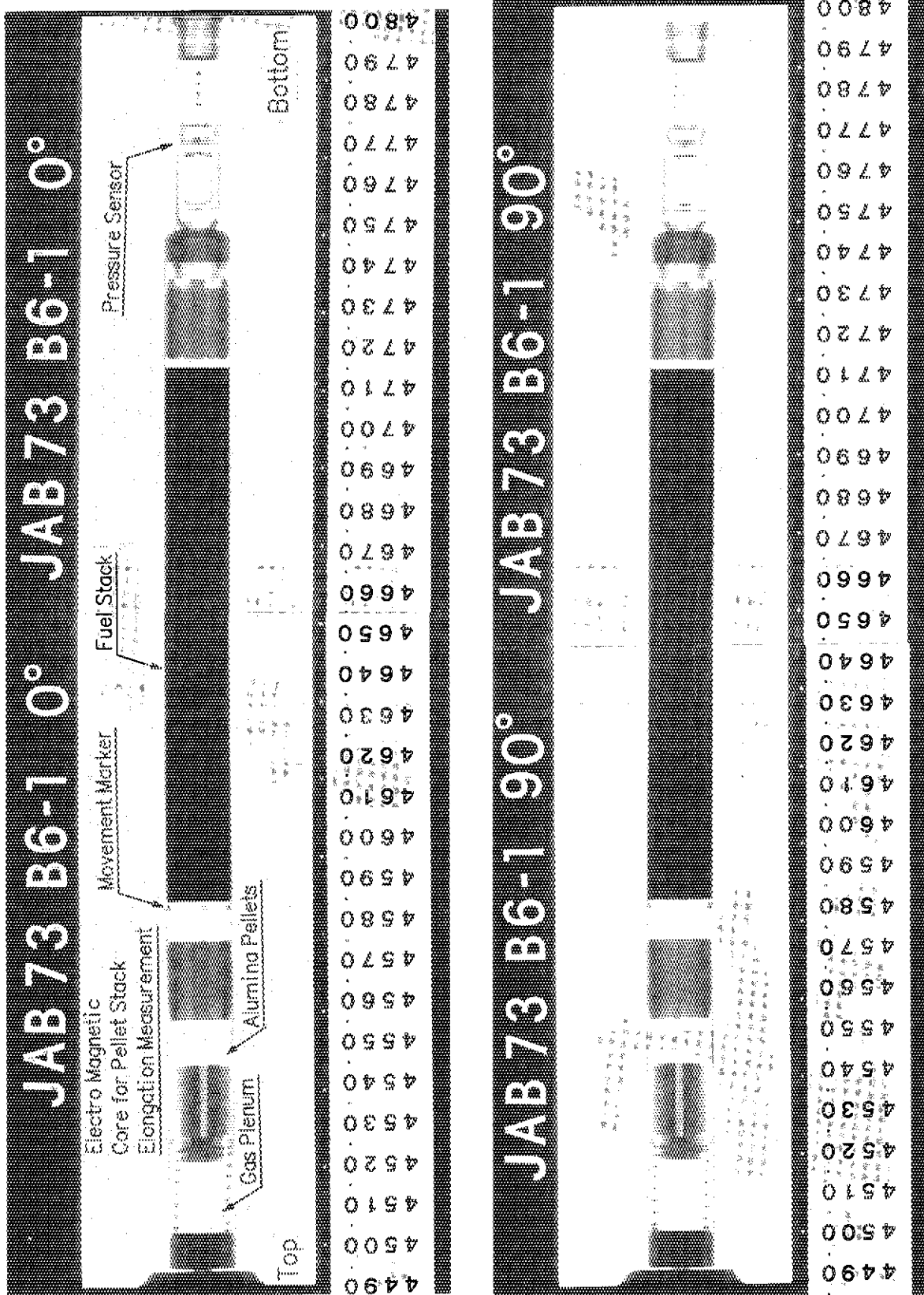
Photo. 2   X-ray radiographs of test fuel rod provided for Test TS-1 (Before pulse irradiation)

Polished

Etched

Polished

Etched

TSURUGA JAB73/B6	MC1	
Without Pulse Irradiation		
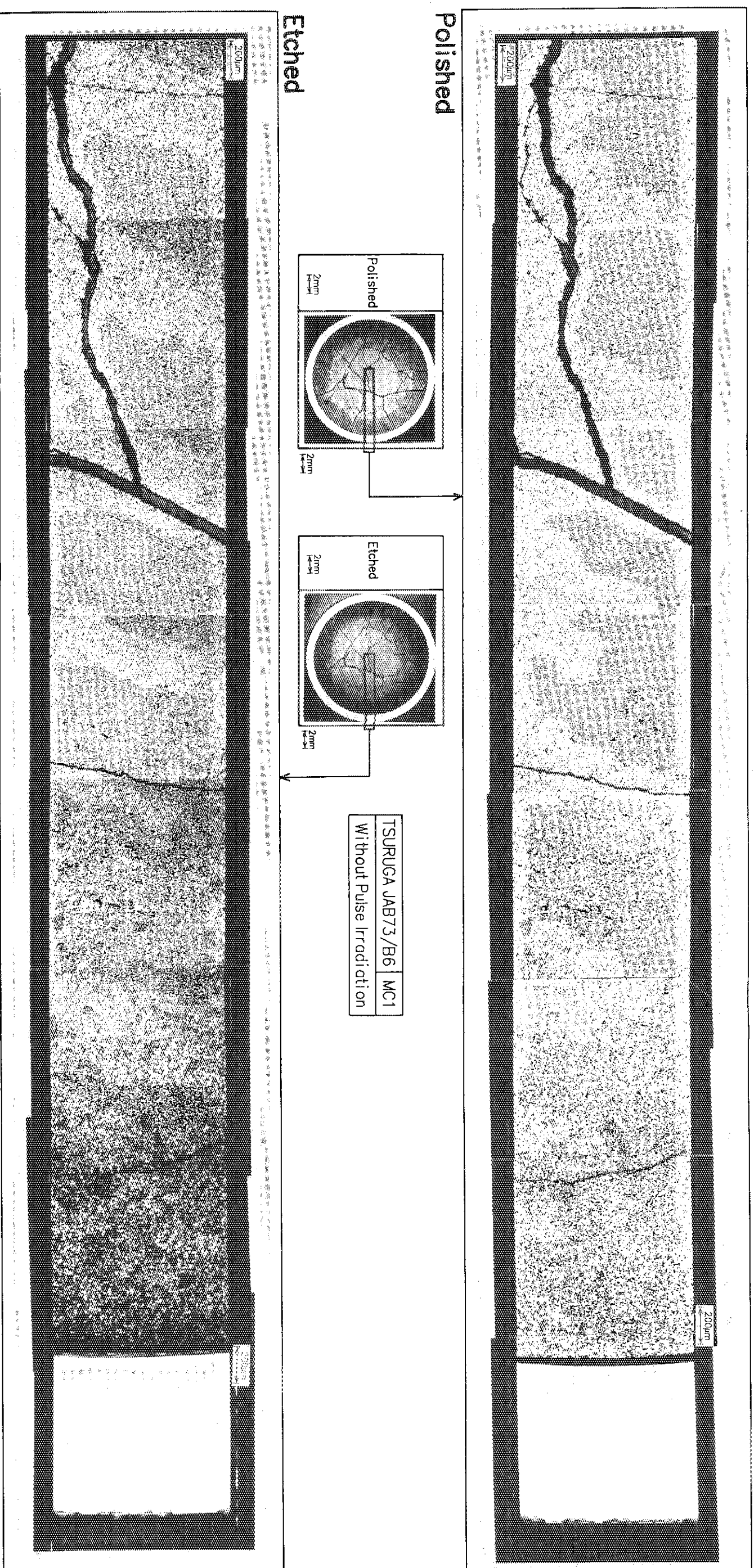
Photo. 5　Enlarged views of radial cross section of irradiated BWR fuel provided for TS tests
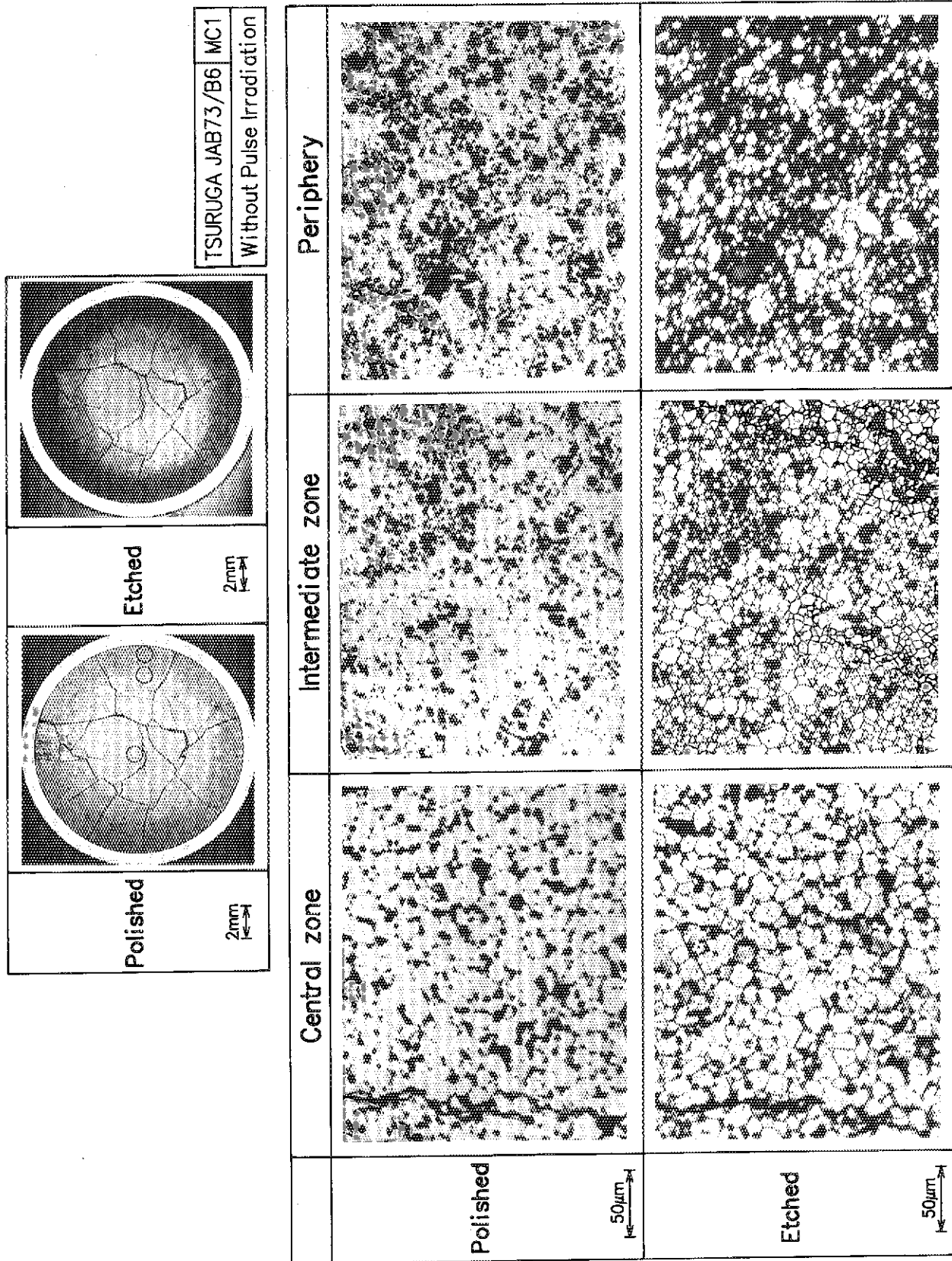
Photo. 6 Micro structure of irradiated BWR fuel pellet provided for TS tests
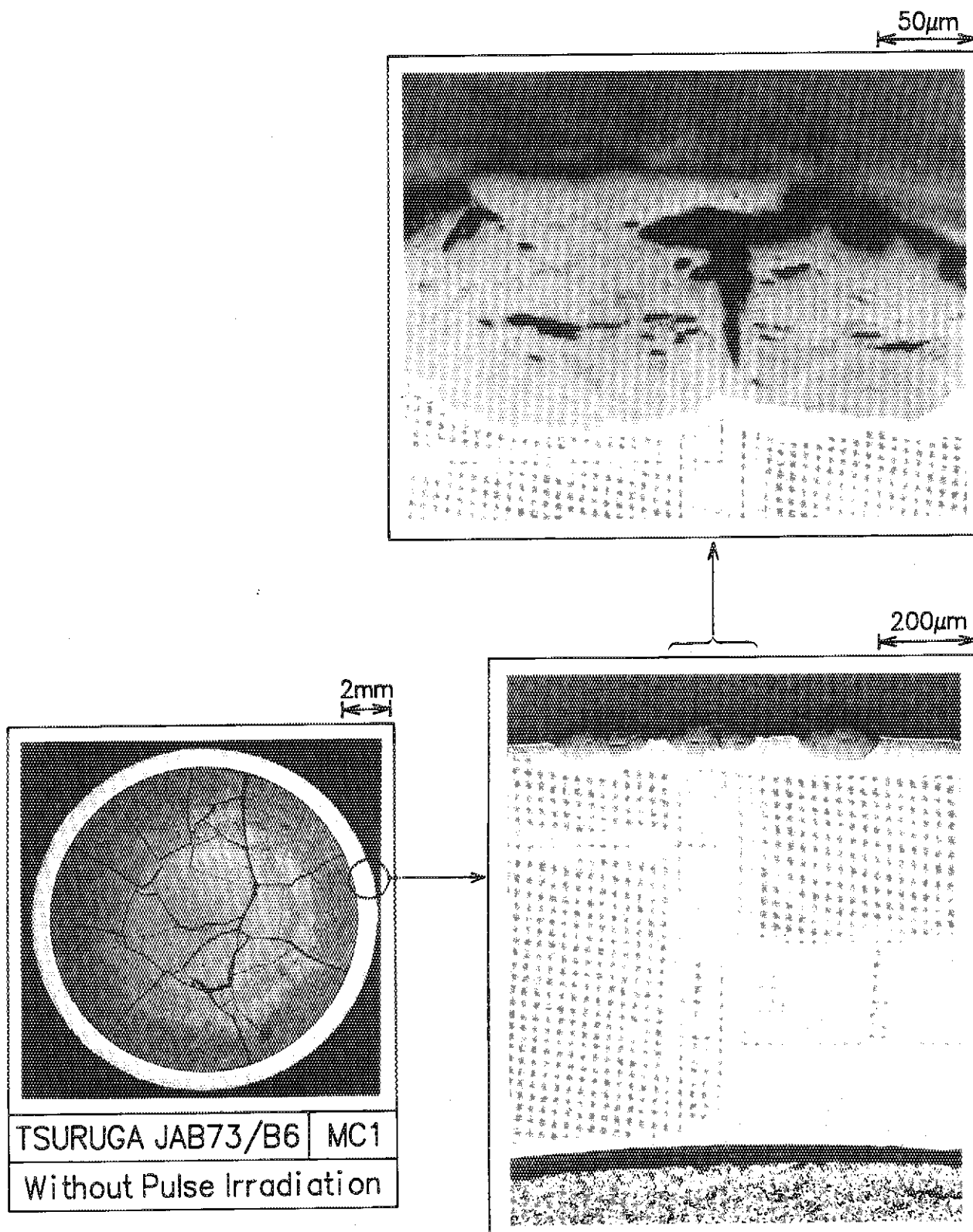
Photo. 7 Examples of nodular corrosions on outer surface of cladding provided for TS tests (Polished)
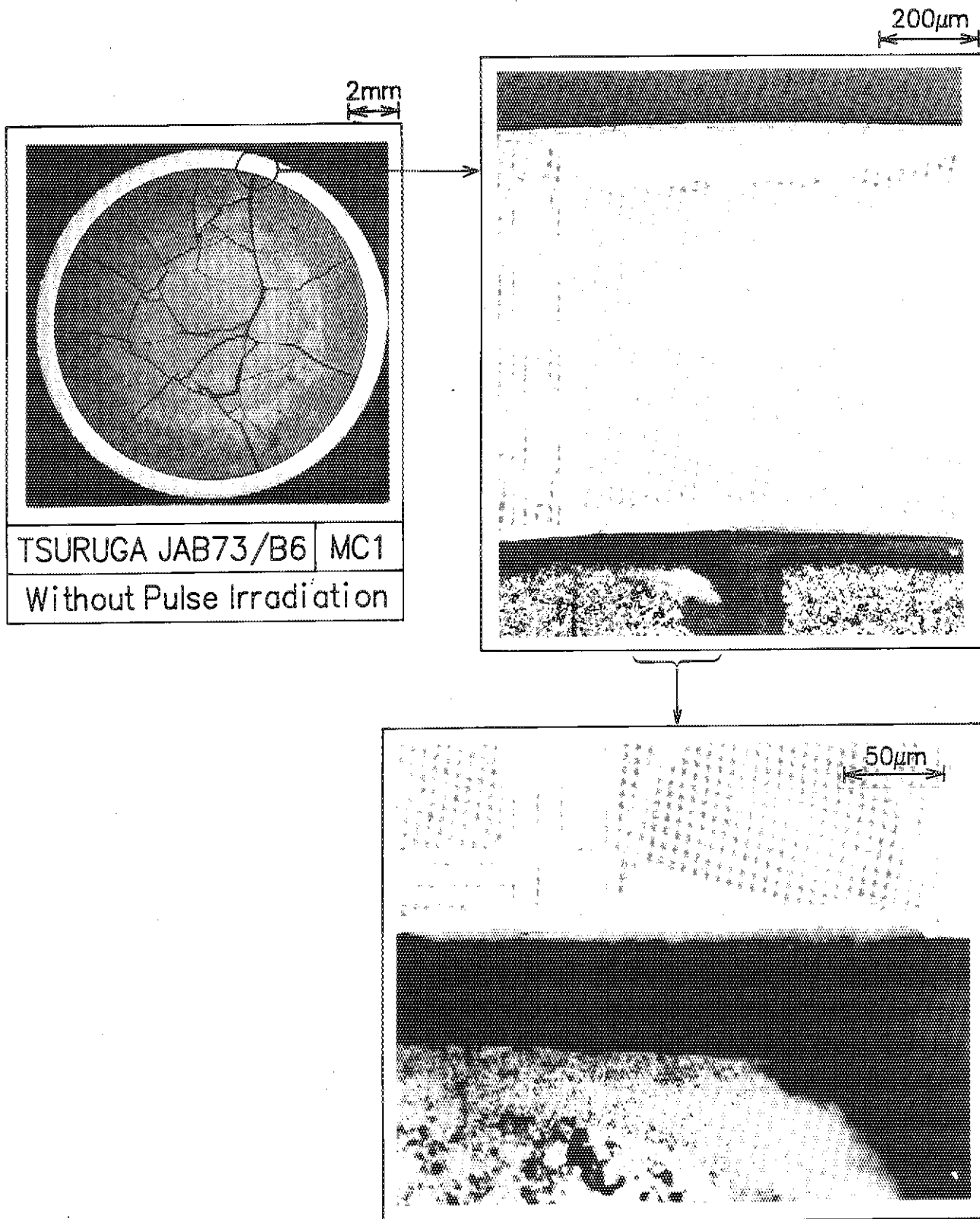
Photo. 8   Example of thin layer of oxide on inner surface of
cladding provided for TS tests (Polished)
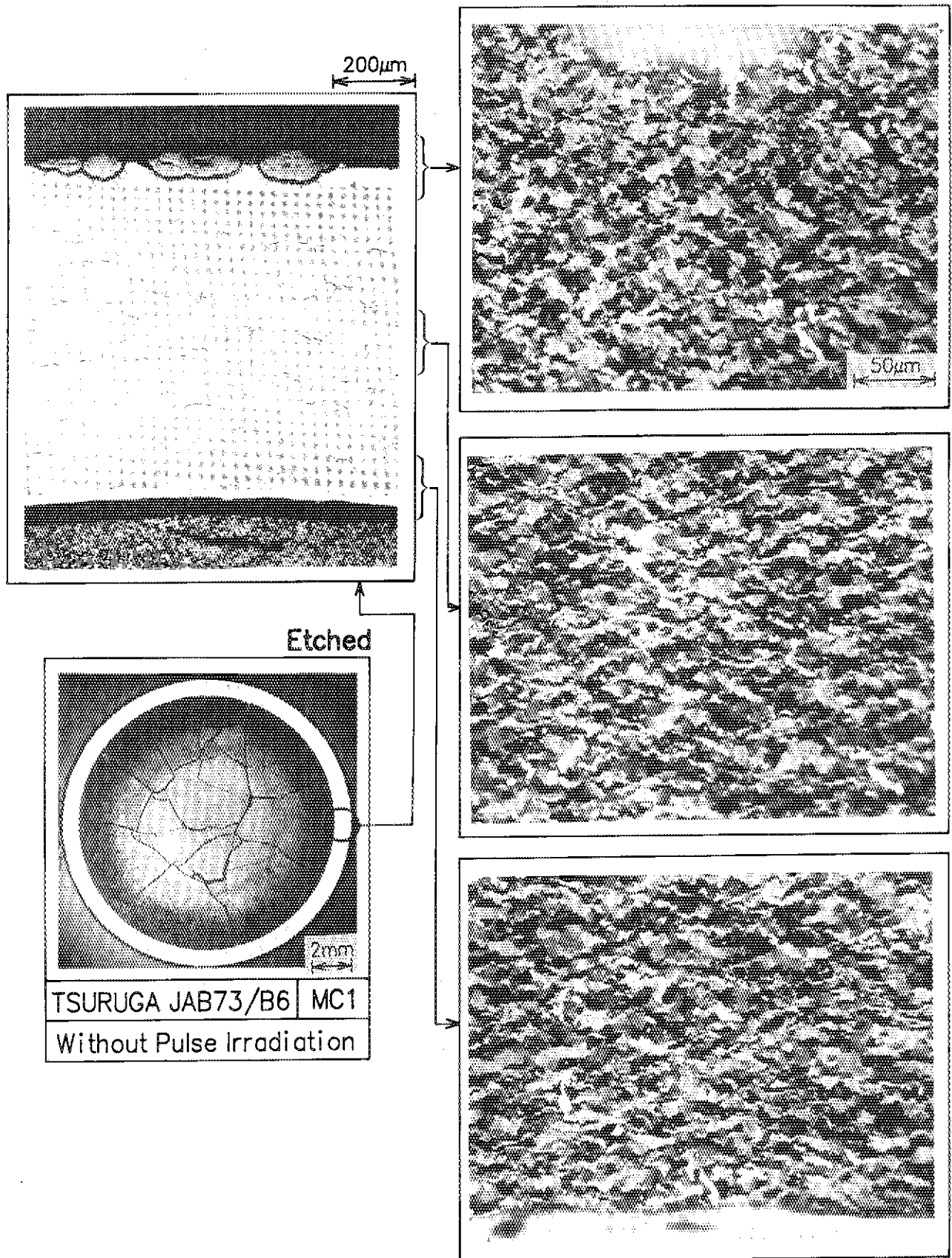
Photo. 9 Hydride distribution and grains of cladding
provided for TS tests (Etched)

TSURUGA JAB73/B6   Without Pulse Irradiation
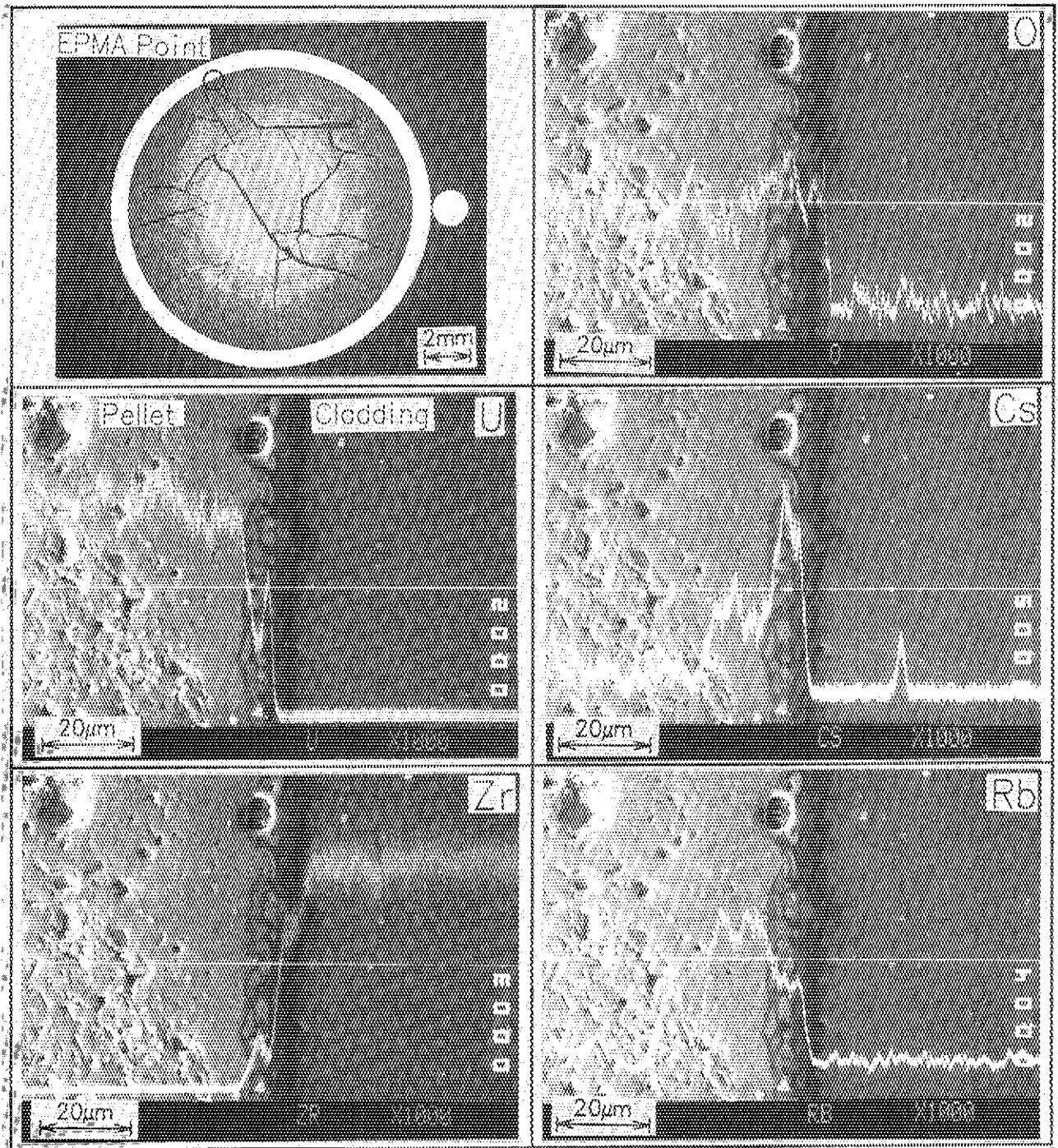
Photo. 10   EPMA analysis results of test fuel without pulse irradiation
(Line analysis)

TSURUGA JAB73/B6   Without Pulse Irradiation
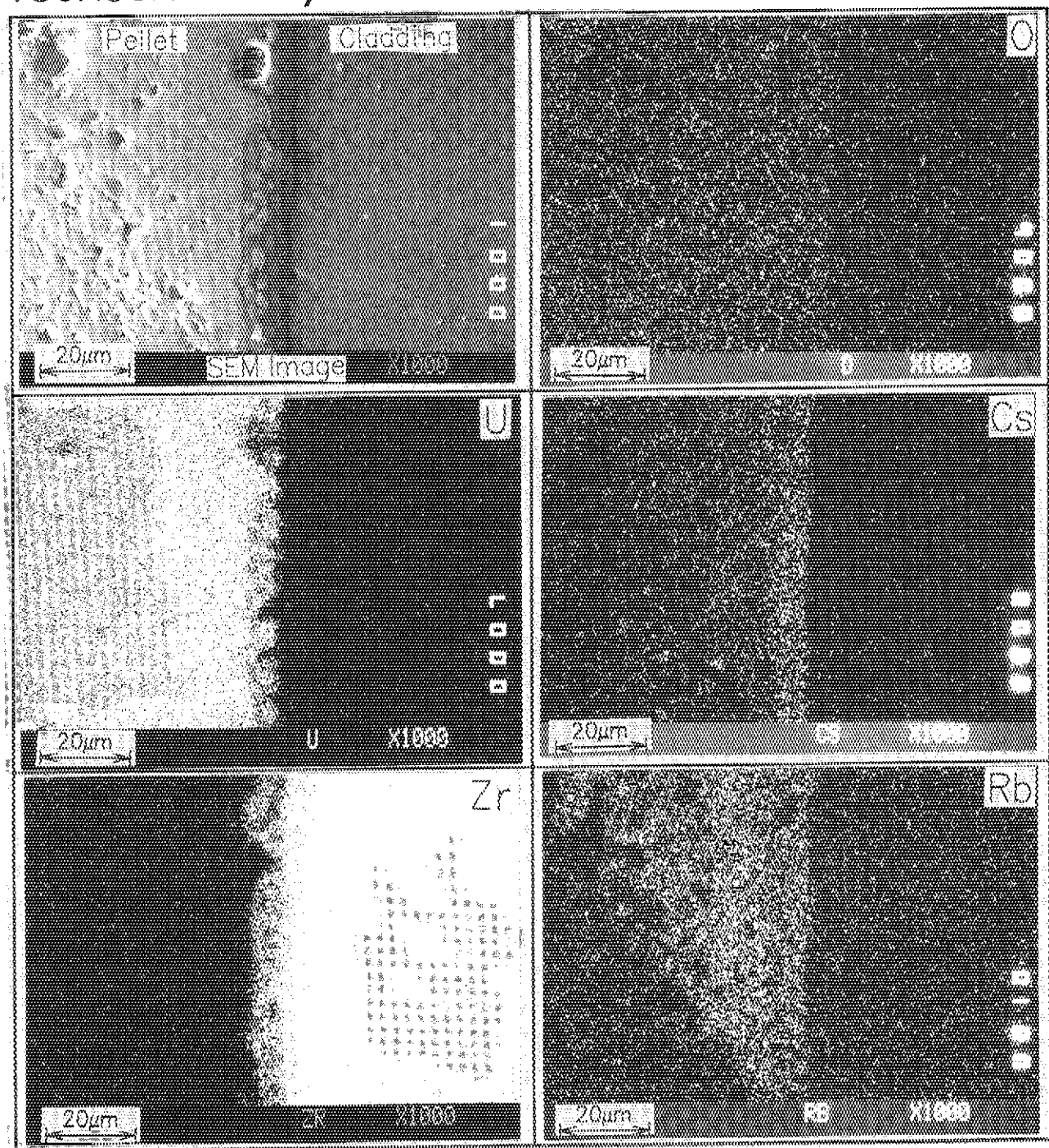
Photo. 11   EPMA analysis results of test fuel without pulse irradiation
(Area analysis)

Without Pulse Irradiation   TSURUGA
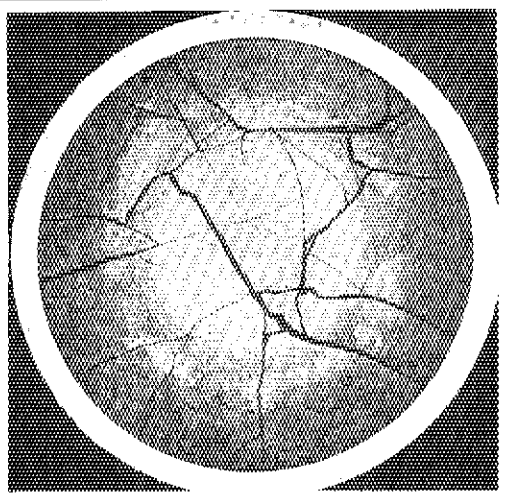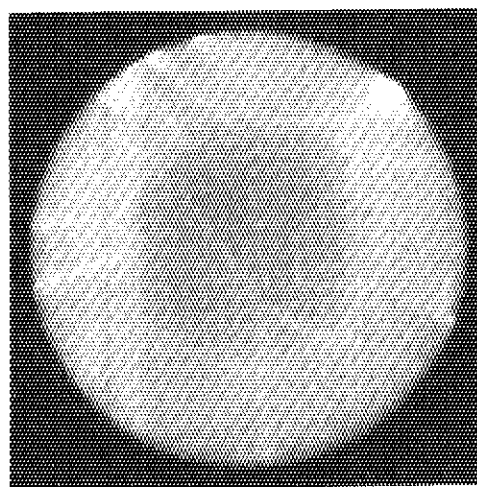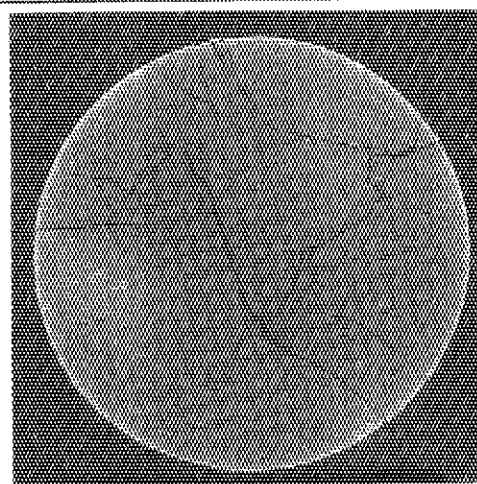
Photo. 12 Auto-radiographs of a cross section sample of
irradiated BWR fuel provided for TS tests

TS-1 After Pulse Irradiation
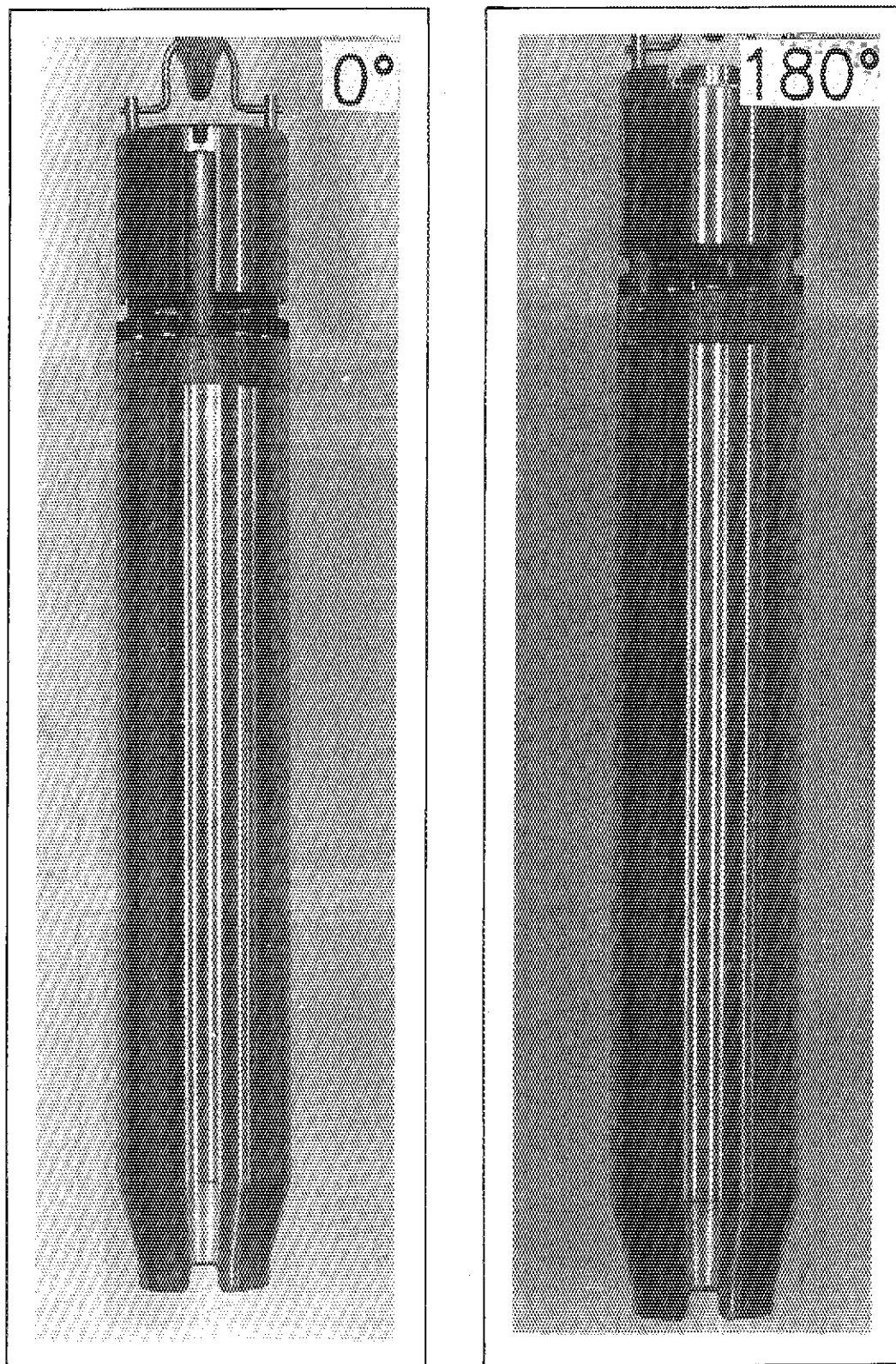
Photo. 13 Appearance of inner test capsule pulse irradiated
in Test TS-1

TS-1 After Pulse Irradiation
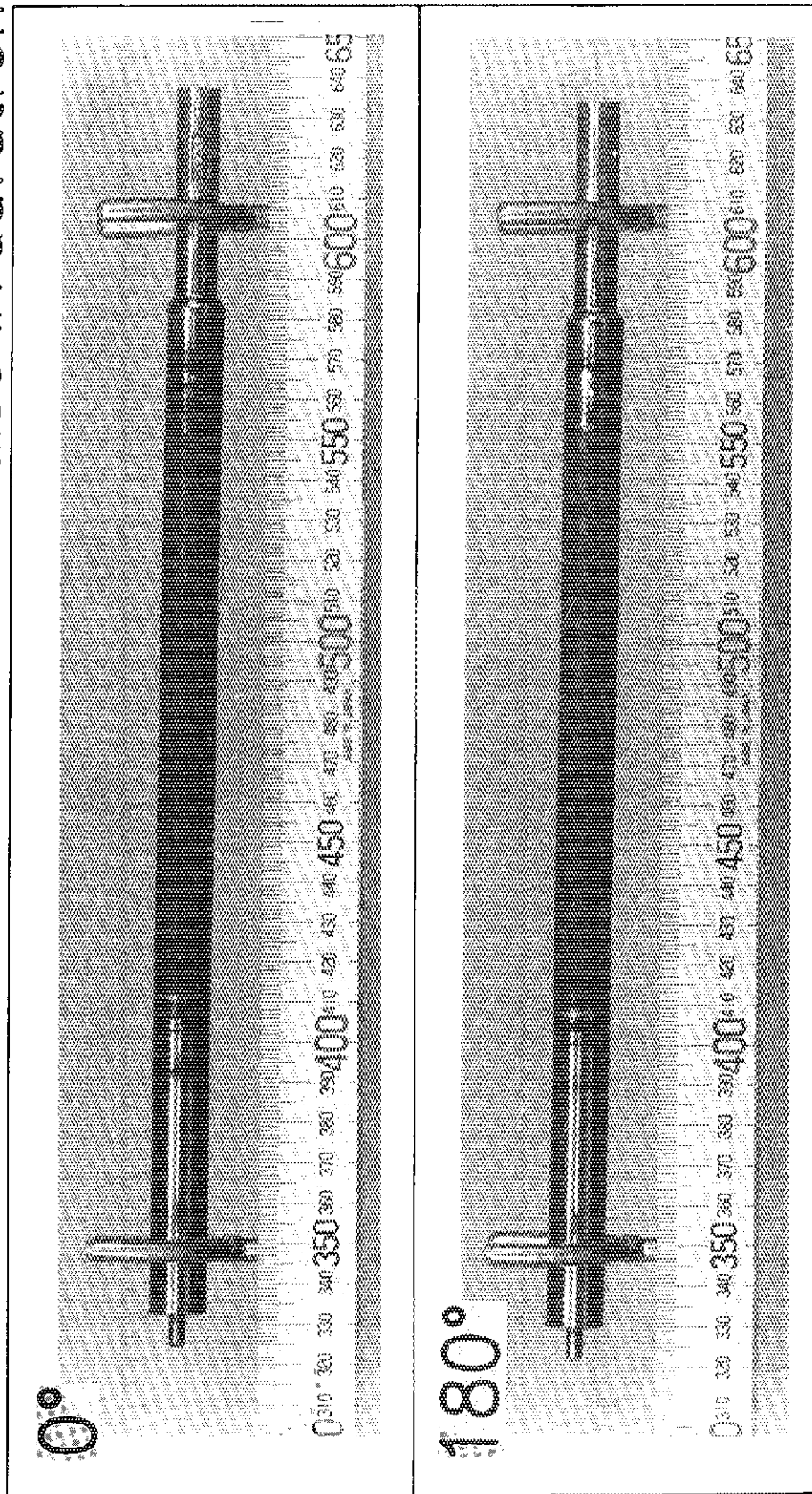
Photo. 14 Appearance of test fuel rod pulse irradiated in Test TS-1
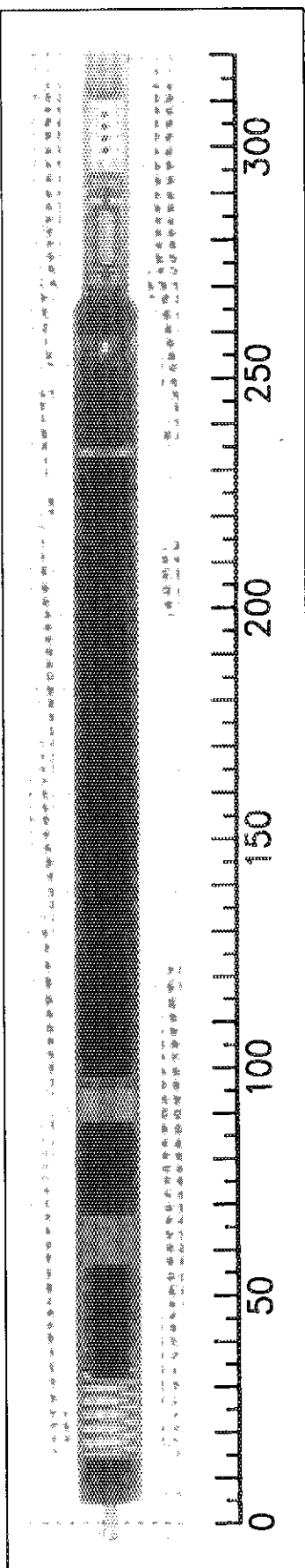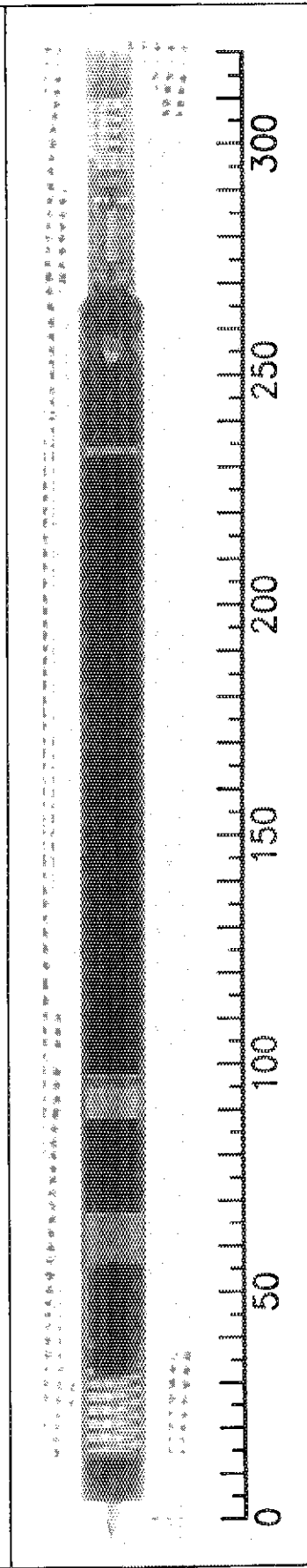
Photo. 15 X-ray radiographs of test fuel rod pulse irradiated in Test TS-1
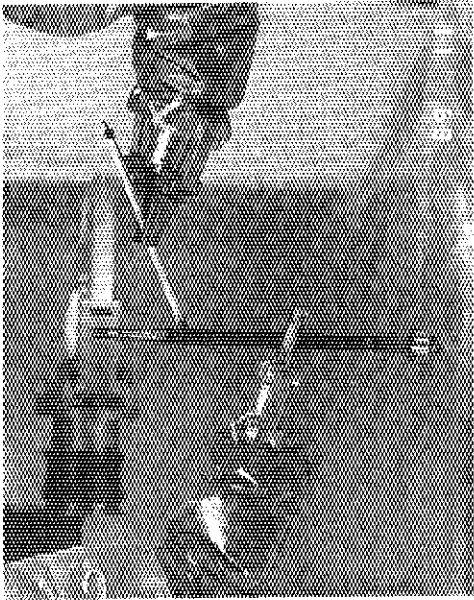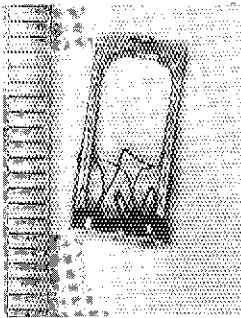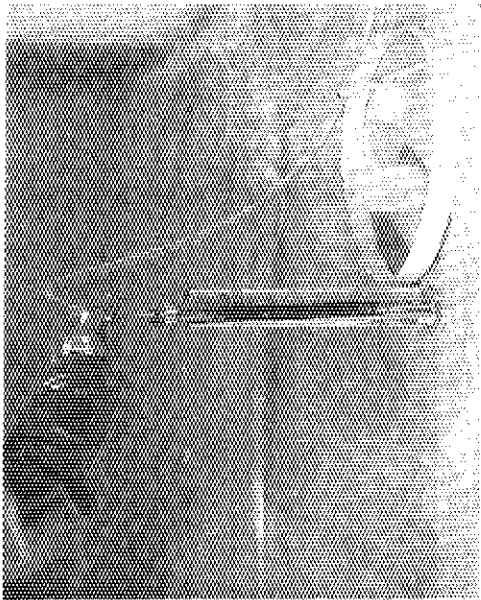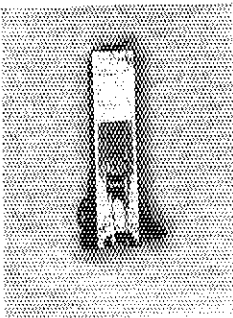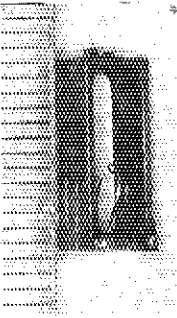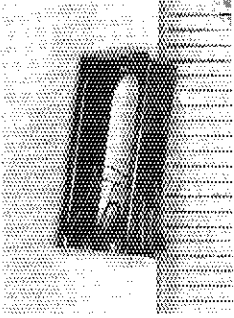
Photo. 16 Leak test of TS-1 test fuel rod and appearance of strain gauges used for pin pressure sensor

TS-1 After Pulse Irradiation

1mm
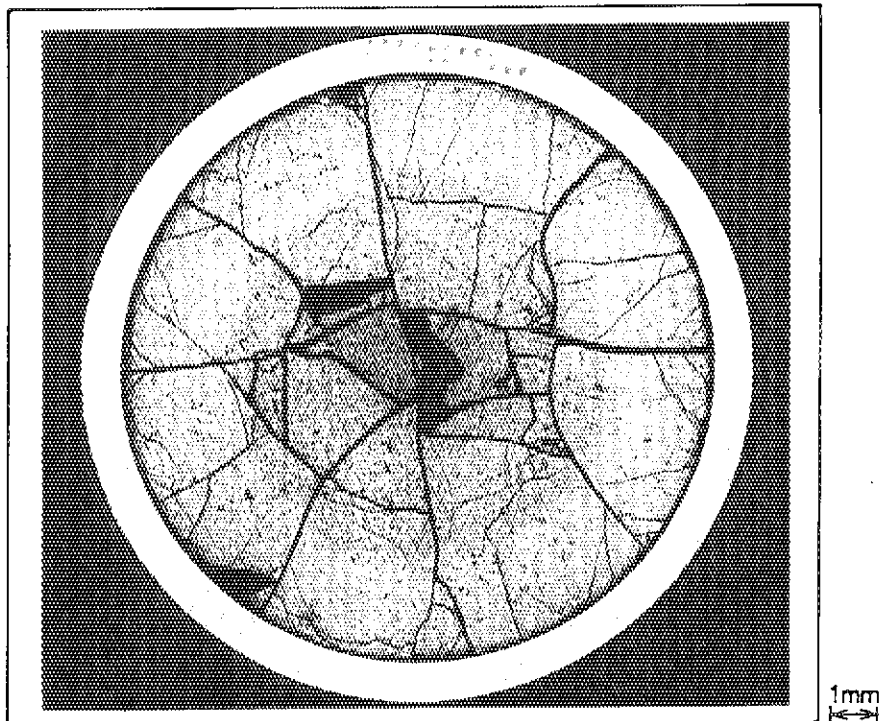
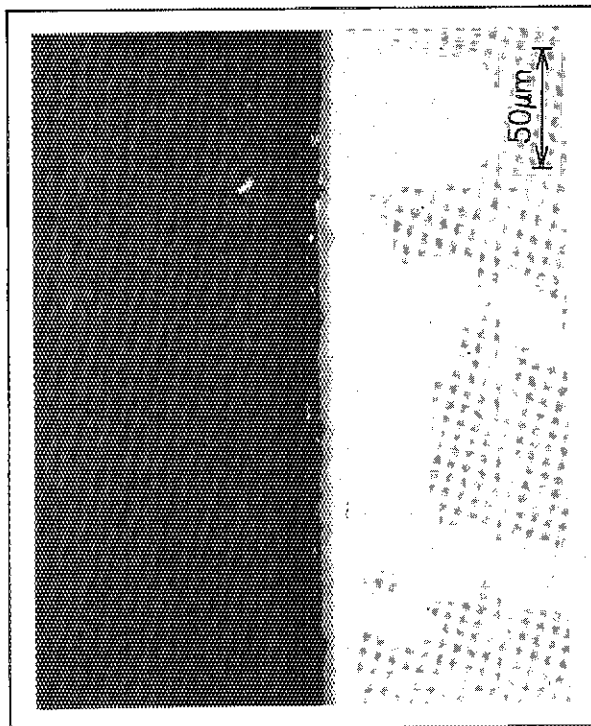Photo. 17   Radial cross section of pulse irradiated test fuel
in Test TS-1 (Polished)

TS-1 After Pulse Irradiation

1mm
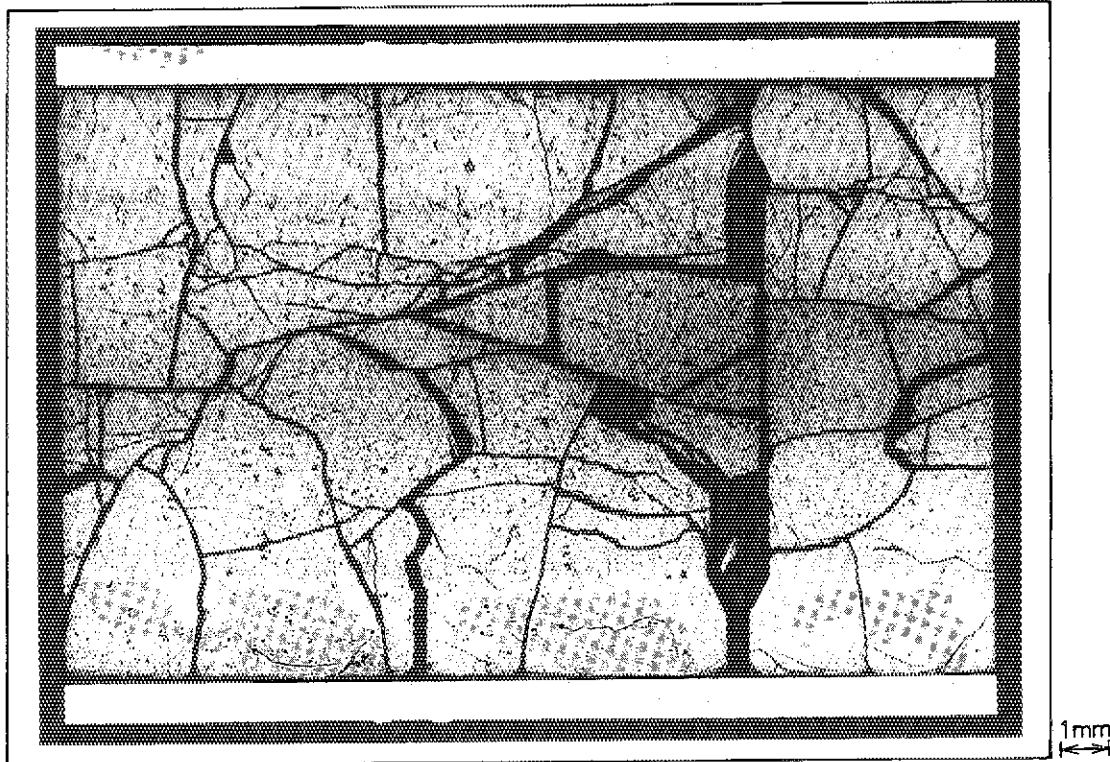
Photo. 18   Axial cross section of pulse irradiated test fuel
in Test TS-1 (Polished)
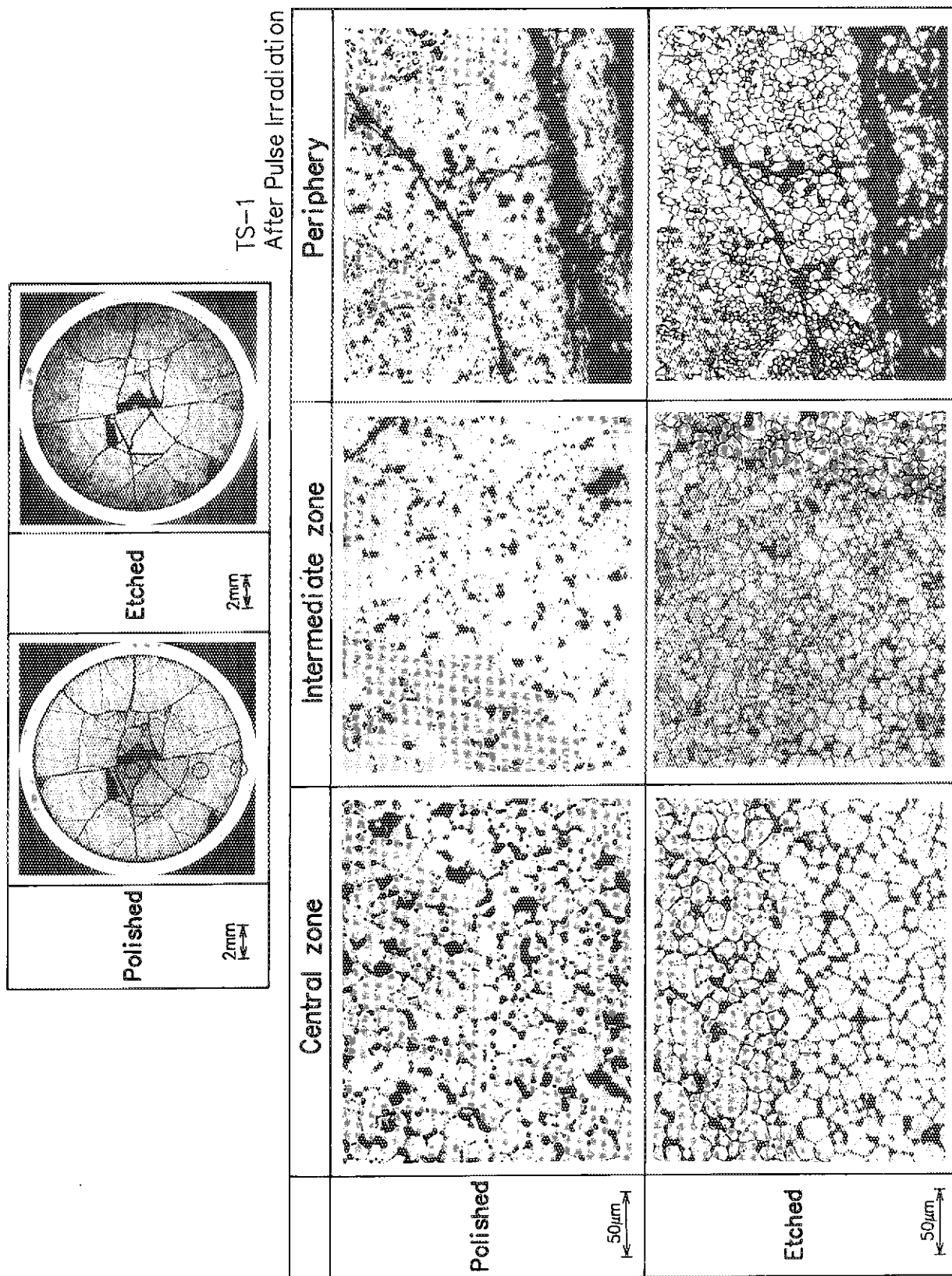
Photo. 19 Micro structure of test fuel pulse irradiated in Test TS-1
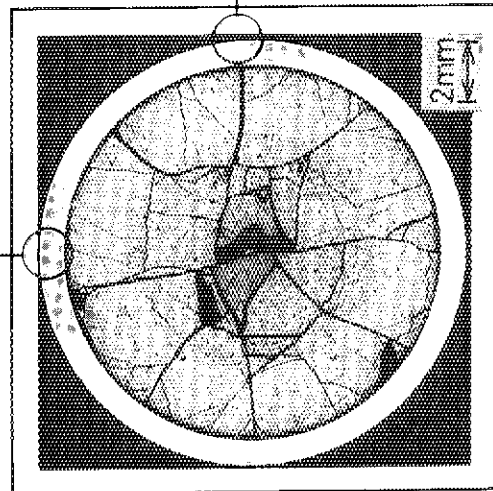
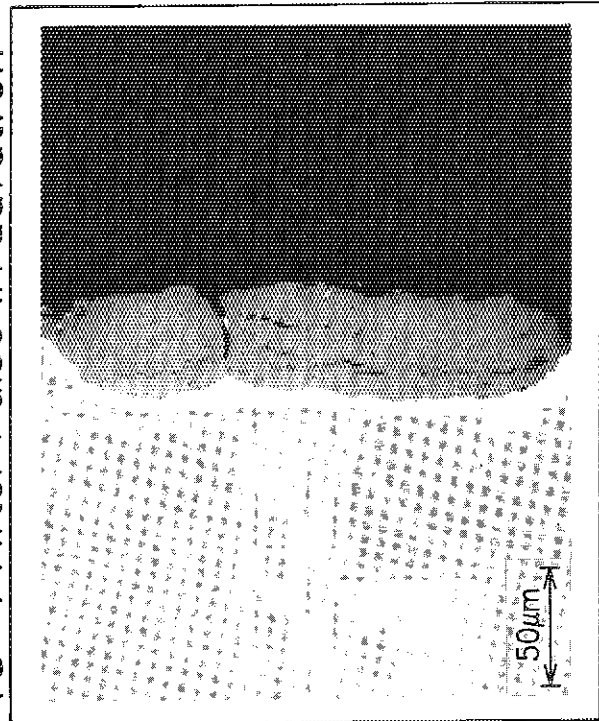TS—1 After Pulse Irradiation

Photo. 20 Corrosions observed on cladding outer surface test fuel rod pulse
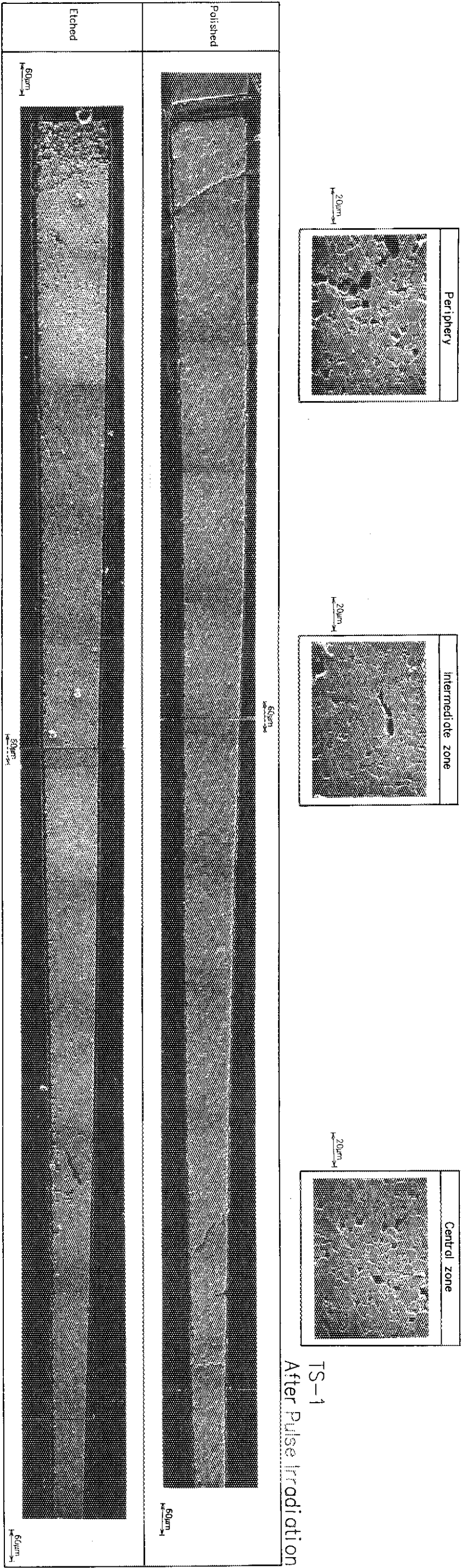irradiated in Test TS—1 (Polished)

Photo. 21 SEM micrographs of a part of radial cross section pulse irradiated in Test TS-1